

NASW-4435

11-51

204231

72P

Bioregenerative Life Support Systems for Microgravity

EGM 4001 Engineering Design
Department of Aerospace Engineering, Mechanics and
Engineering Science
University of Florida

April 1993

(NASA-CR-195516) BIOGENERATIVE
LIFE SUPPORT SYSTEMS FOR
MICROGRAVITY (Florida Univ.) 72 p

N94-24810

Unclass

G3/51 0204281

EGM 4001

ENGINEERING DESIGN II

Bioregenerative Life Support Systems for Microgravity

Prepared for

National Aeronautics and Space Administration
Kennedy Space Center, Florida

and

Universities Space Research Association

April 1993

Prepared by

EGM 4001 Engineering Design
Department of Aerospace Engineering,
Mechanics and Engineering Science

University of Florida
Gainesville, Florida 32611
(904) 392-0961

Professor

Dr. Gale E. Nevill, Jr.

Teaching Assistants

Michael I. Hessel, Jr.
Jose Rodriguez

Editor

Steve Morgan

Class Members

Scott Breneman
Jeff Burke
Mark Cates
Mark Dallara
Randy Hines
Tu-Ming Leung
Steven Morgan
Margaret Olson
Tom Rossi
Kathryn Samuels
Michael Schreiner
Ed Solozabal
Jeff Yang

To all those who aided and assisted us:

Dennis Chamberland
Principal Contact with NASA

Harold Doddington
Use of Electronic Lab use, and technical advice

Micro Switch
Donation of Hall Effect Sensors

Permag Corp.
Donation of Ceramic Magnets

Art Taylor
Slides

Dr. Anna Toth
General chemistry information

Donna Turner
Equipment

Dr. Vaneica Young
Information about ion selective electrodes

Dr. Ralph Prince
For a little bit of lettuce inspiration
and especially the NASA CELSS project

Thank you.

Table of Contents

Aqueous Nutrient Solution Sensor Project	1
A Variable Geometry Plant Growth Unit	14
Mass Determination Device	28
Variable Lighting System	50

Aqueous Nutrient Solution Sensor Project

**Mark Dallara
Randy Hines
Scott Breneman**

Table of Contents

INTRODUCTION	3
BACKGROUND/THEORY	3
APPLICATION OF THEORY	5
CALIBRATION ROUTINE	5
EQUIPMENT AND MATERIALS	6
<u>Chemicals</u>	6
<u>Ion Selective Electrodes</u>	6
<u>Thermistor</u>	7
<u>A/D Board</u>	7
EXPERIMENTAL PROTOCOL	7
RESULTS	9
ANALYSIS	10
WORKS CITED	13

INTRODUCTION

NASA's Controlled Ecological Life Support System (CELSS) project centers on growing plants and recycling wastes in space. The current version of the Biomass Production Chamber (BPC) uses a hydroponic system for nutrient delivery. To optimize plant growth and conserve system resources, the content of the nutrient solution which feeds the plants must be constantly monitored. The macronutrients (>10 ppm) in the solution include nitrogen, phosphorous, potassium, calcium, magnesium, and sulphur; the micronutrients (<10 ppm) include iron, copper, manganese, zinc, and boron.

The goal of this project is to construct a computer-controlled system of ion detectors that will accurately measure the concentrations of several necessary ions in solution. The project focuses on the use of a sensor array to eliminate problems of interference and temperature dependence.

BACKGROUND/THEORY

In developing a sensor array to accomplish these goals, several sensor types have been examined. The most promising was judged to be Ion-Selective Electrodes (ISE). An ISE is a sensor electrode with material at one end that only allows certain ions to react electrochemically to the probe. An ISE is paired with a reference electrode and the voltage difference between the two is related to the concentration of the ion of interest by the Nernst Equation:

$$E = E_O + ST \cdot \log(a) \quad (1)$$

Figure 1 illustrates the actual response for a typical ISE. The transfer function exhibits a linear range in which the electrode behaves according to the Nernst equation, preceded by a low-level non-linear range. The solutions measured in this project were well within the linear range of the electrodes.

Ideally, an ISE would only react with the selected ion, however most ISE's fall short of this goal. The voltage difference is also affected by the presence of other ions and changes in

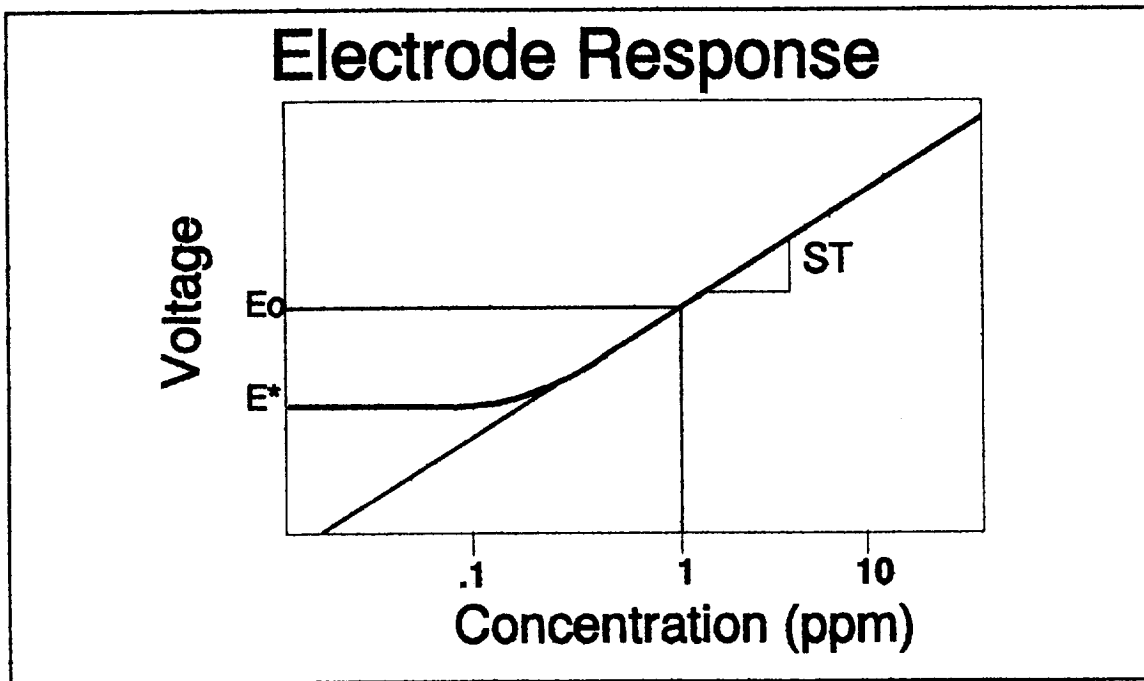


Figure 1

temperature and pH. The primary effort of our project was to account for these influences in the performance of the sensor system.

Electrochemical analysis of ISE theory produces a theoretical relationship between the voltage of the ISE and the reference electrode, which is represented by the Nikolskii-Eisenmann equation:

$$E = E_0 + \frac{RT}{Fz_1} \log(a_1 + \sum_{k=2}^n K_{1k} a_k^{z_1/z_k}) \quad (2)$$

where E is the measured voltage, E_0 is the standard voltage at a unit concentration, R is the universal gas constant, F is Faraday's constant, and z_1 is the charge of the selected ion. The summation is over the other k ions in the solution. K is an interference coefficient and z the charge of each ion. The symbol a is the activity of the ion and is directly related to the concentration of the ion.

Not all ions interfere with each ISE so some of the K 's are zero. At low concentrations, similar to those found in plant nutrient solutions, the activity of the ion (a) is equal to its concentration. The interference coefficients (K_i) may also vary with temperature.

APPLICATION OF THEORY

The first step of the project was to prepare a data acquisition program to coordinate and use information from each electrode. The program included procedures for calibration, sampling, and the calculation subroutine which produced "first-guess" Nernstian values for concentration as well as the iterative solution based on the Nikolskii-Eisenmann equations. Once this was functional, the electrodes were calibrated and the interference constants were determined experimentally. The system was then ready to test samples with multiple ions.

CALIBRATION ROUTINE

Calibration of any particular electrode involves the determination of the constants E_0 and $S = \frac{R}{Fz}$ as found in the Nikolskii-Eisenmann equation.

Since these tests are carried out using only the ion for which that particular electrode is selective to, the values of the activity for all other ions (a_k) must equal zero.

Calibration of each sensor begins by choosing the range over which sample data will be taken. Two samples are taken of solutions with different activities a_1 and a_2 , such that $a_1 = 10^n a_2$. It should be realized that the subscripts on the concentration (a) refer to different concentrations of the same ion, and not concentrations of two different ions. The two Nernstian equations which result from these samples are:

$$E_1 = E_0 + ST \cdot \log(a_1) \quad (3)$$

$$E_2 = E_0 + ST \cdot \log(a_2) \quad (4)$$

These can be solved simultaneously to find ST:

$$ST = \frac{E_2 - E_1}{\log(a_2) - \log(a_1)} \quad (5)$$

E_0 can be found by back substitution. The computer program used in this system carries out these calculations and saves the new calibration constants automatically. Calibration concentrations of 100 parts per million (ppm) and 1000 ppm were used to calibrate each electrode.

EQUIPMENT AND MATERIALS

Chemicals

The choice of the chemicals used came from consideration of the nutrients in the solution as well as the availability of ion selective electrodes. Since the worst problem with using ISEs is the error caused by interferant ions, the chemicals were intentionally chosen to cause maximum interference. Nutrient solutions for plant growth include calcium and potassium, both of which have commercially available electrodes. Both of these electrodes experience interference from sodium ions. Although sodium is not found in nutrient solutions, its presence as an interfering ion was important for the experimental procedure. The chemicals used will be calcium chloride dihydrate, potassium chloride, and sodium chloride.

Ion Selective Electrodes

Three Orion ISE's comprised the array. They consisted of two liquid membrane electrodes and one glass membrane electrode. The two liquid membrane electrodes (calcium and potassium) were referenced to a double junction reference electrode using the standard inner-chamber fill solution. The outer-chamber fill solution was chosen because it allowed both the calcium and potassium electrodes to function normally. Using ammonium chloride solution (2M NH_4Cl) instead of the more common potassium nitrate solution (10% KNO_3) decreases the amount of

interference in each electrode as the outer fill solution slowly seeps through the semi-permeable membrane of the double junction electrode.

Thermistor

An Omega 44008 Linear Thermistor Composite was used for temperature measurements. The wires of the thermistor have been covered with a plastic dip to avoid contact with the solution. The thermistor is used in conjunction with a bridge circuit that provides the output voltage to be read by the A/D board.

The temperature range of the thermistor is from -40 C to 150 C which is more than adequate for ion sensing. Accuracy of the thermistor at temperatures ranging from 10 C to 50 C (well within testing specifications) is ± 0.2 C.

A/D Board

The A/D board used is the DASCON-1 by MetraByte. The DASCON-1 has a four channel, 12 bit analog to digital converter. The board measures ± 2.0475 volts with resolution of 0.0005 volts. The A/D board has been tested for its precision of measurements on channels 0-3. The measurements were consistent on all four channels with a precision of ± 1 millivolt.

EXPERIMENTAL PROTOCOL

After calibration of each electrode, each interference constant (K_{ij}) was determined by testing a solution which contained 100 ppm test ion and 1000 ppm interference ion. For the purposes of this project, these values were assumed to be constant for all temperatures during the life of the electrode. The calibration constants were subject to change, depending on the most recent calibration.

When running the program, the user input the known concentrations of each ion in the test solution and the A/D board then began sampling. The four data channels corresponded to

the voltage output of each of the electrodes and the thermistor bridge circuit. When a sampled data channel appeared to stabilize, the user "held" the value by pressing the key for that channel and the held value was displayed below the free-floating value. Once all values were held, the user exited sample/hold mode and the program calculated and output the Nernstian "first-guess" value and the iterative value of each concentration.

The testing scheme was as follows:

	Na (ppm)	Ca (ppm)	K (ppm)
Test 1	100	1000	0
Test 2	100	1000	1000
Test 3	1000	1000	0
Test 4	1000	1000	1000
Test 5	0	100	1000
Test 6	1000	100	1000
Test 7	1000	0	100
Test 8	1000	1000	100

Ionic strength adjustor (4M NH_4Cl 4M NH_4OH) was necessary for the sodium electrode in the ratio of 1 mL ISA per 10 mL test solution. The calcium electrode functioned equally well with or without ISA, so none was used.

The potassium electrode functioned well when used with ISA (5M NaCl) during initial calibration, but upon successive recalibrations the electrode slope was found to have decreased to 1 mV/decade. No amount of reconditioning changed the slope and the potassium electrode had to be discarded as a data source. The program was altered to produce a simulated data reading based on the "known concentration" inputs and the Nikolskii-Eisenmann equation. Therefore, the data output for the potassium electrode potential is a trivial value, but its effect on the calculations of the sodium and calcium ion concentrations could still be examined.

Between tests the sodium electrode was rinsed with a solution of 0.04 M NH_4Cl and 0.04 M NH_4OH ; the calcium electrode was rinsed with deionized water. When not in use, the

electrodes were stored in a 100 ppm solution of their respective ions. The reference electrode was stored in deionized water.

RESULTS

Figures 2 and 3 below illustrate the Nernstian output and the Nikolskii-Eisenmann iterative output as compared to the real concentration of the ion for calcium. Results for sodium were similar, but generally less accurate.

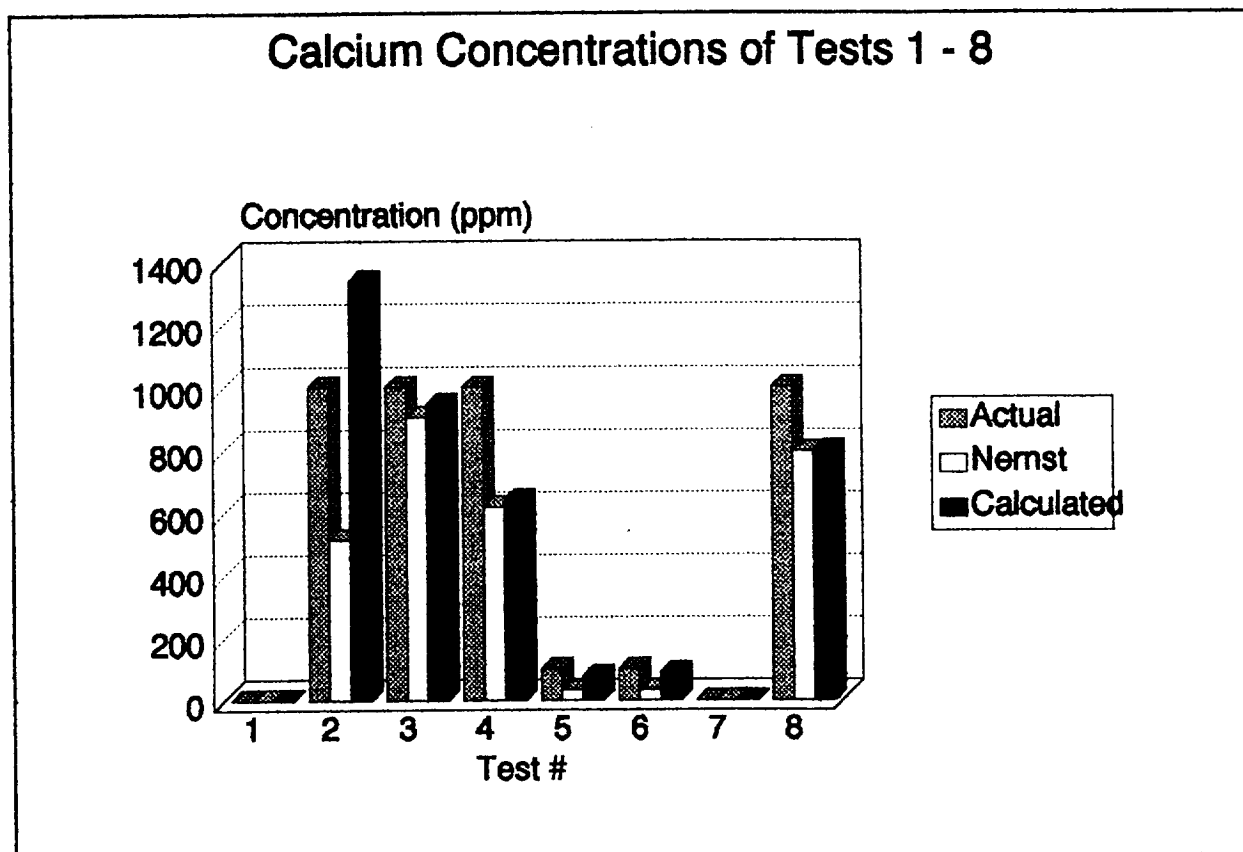


Figure 2

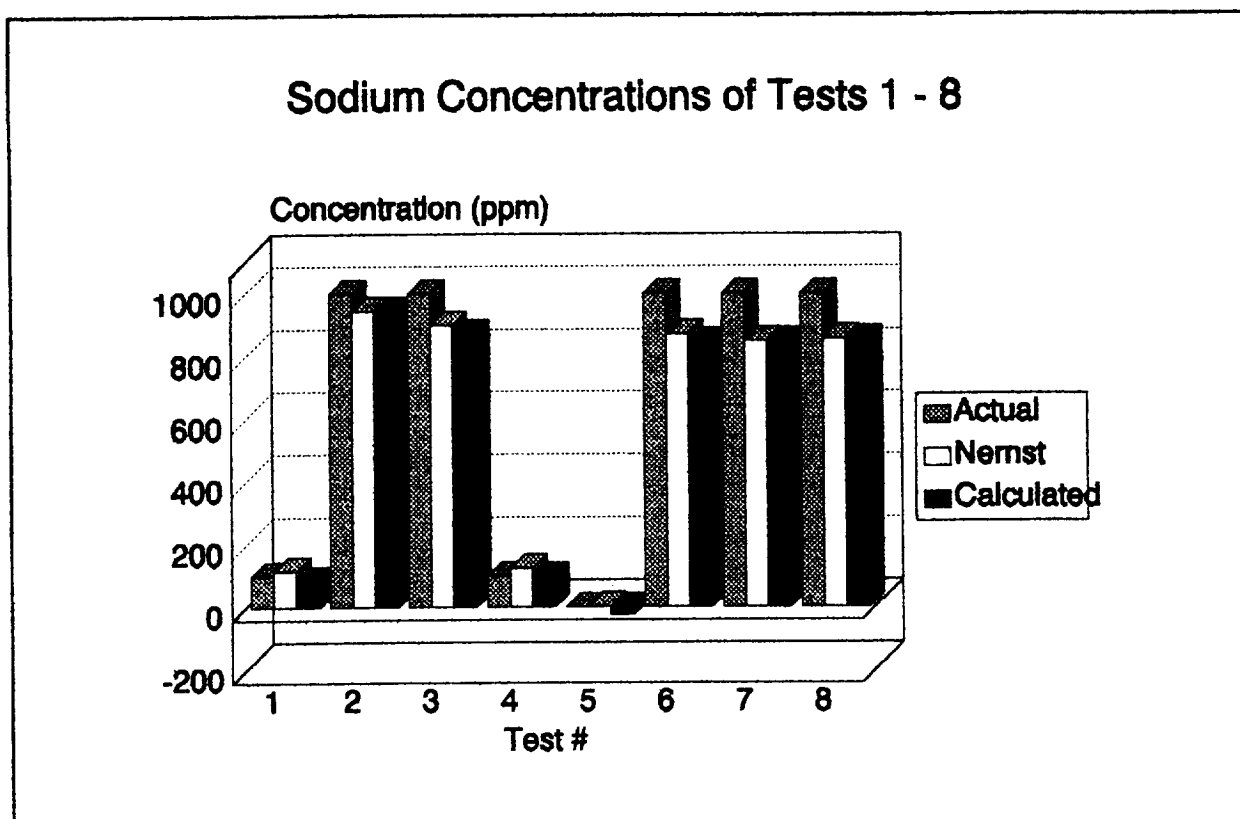


Figure 3

ANALYSIS

The iterative procedure presented in this project produced mixed results. The differences between the single-electrode outputs and the array outputs were different for each electrode. The values for calcium concentration tended to be more accurate, while the values for sodium tended to be less accurate. As noted above, the potassium electrode had an insufficient response function and had to be discarded as an input.

The errors evident in some of the output values could be attributed to several different sources. As shown in Figures D and E below, a small difference in the calibration constants produces a rather large difference in both the Nernstian output and the Nikolskii-Eisenmann output.

Sensitivity of Calcium Output to Change in Electrode Slope

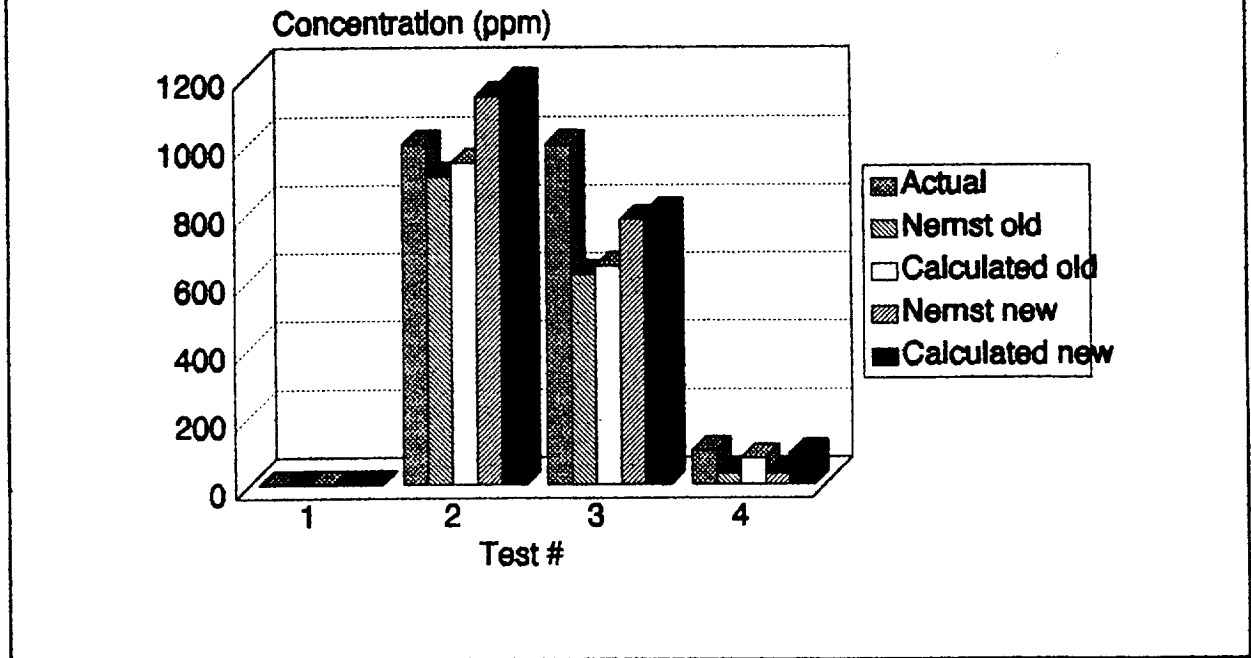


Figure 4

Additional errors may have been introduced by inaccuracies in the output from the A/D board or the thermistor bridge circuit. All of these values (calibration constants, voltage outputs, and temperature) are part of the exponent in the Nernst equation when solved for concentration:

$$a_1 = 10^{\frac{E_1 - E_0}{ST}} \quad (6)$$

Thus both the Nernst and the Nikolskii-Eisenmann outputs are strongly sensitive to the calibration values as well as the accuracy of the voltage and temperature readings.

A multiple-input array may be applied to any situation in which the individual sensor outputs are imprecise and interrelated.

The ion selective electrodes used here proved to be temperamental devices with a number of inherent problems. The need to use ISA for reasonable output negated one of the goals of the project - to test the solution without changing it. Without ISA, the sodium electrode illustrated a response with almost zero slope. The sodium electrode was also

Sensitivity of Sodium Output to Change in Electrode Slope

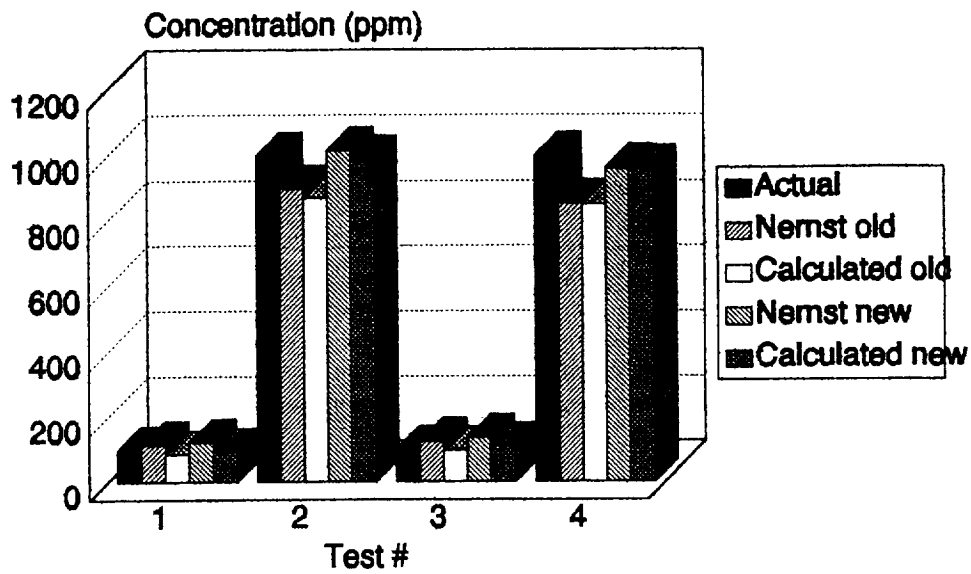


Figure 5

extremely sensitive to static charge in the room; touching the shielded BNC connector caused the voltage output to go to zero, and fluctuations in the output were repeatedly observed due to such minor disturbances as a person walking past the system setup.

It appears that a sensor array may indeed be useful to systems with multiple-ion solutions and imperfect detectors. However, the precision of the associated hardware and the method of sampling and calibration are critical to the procedure; these need to be improved before this system could accurately test a real hydroponics solution.

WORKS CITED

Doddington, Dr. Harold. AeMES Department, University of Florida.

Evans, A. 1987. Potentiometry and Ion Selective Electrodes. New York: John Wiley and Sons.

Schuetzle, D. 1986. Fundamentals and Applications of Chemical Sensors. Washington: American Chemical Society.

Toth, Dr. Anna. Analytical Chemistry Department, University of Florida.

Young, Dr. Veneica. Chemistry Research Department, University of Florida.

A Variable Geometry Plant Growth Unit

**Steven Morgan
Margaret Olson
Kathryn Samuels
Michael Schreiner**

Table of Contents

SUMMARY	16
INTRODUCTION	17
WHY A VGPGU?	17
CURRENT RESEARCH	17
CHARACTERISTICS	18
POSSIBLE DESIGNS	19
<u>Criss-Cross</u>	19
<u>The Telescope</u>	20
<u>The Tracked Wheel and The Wedge</u>	20
<u>The Accordion</u>	21
DESIGN CHOICE	22
FABRICATION	22
<u>Prototype</u>	22
<u>Second Wind</u>	23
<u>The Details</u>	23
EXPERIMENTATION	24
<u>Plants</u>	24
<u>Prototype</u>	24
<u>Results</u>	26
CONCLUSIONS	26
WORKS CITED	27

SUMMARY

With long-term manned space missions now technologically feasible, life supports systems for the astronauts need to become self-sustaining and durable. Such a system would require plants to recycle waste and air. However, in the confined volume of a spacecraft, a unit to grow plants in the least amount of volume necessary would be necessary. This paper introduces a Variable Geometry Plant Growth Unit (VGPGU) developed at the University of Florida.

The VGPGU developed, dubbed the "Accordion" for its resemblance to the musical instrument, is able to stretch and contract and efficiently deliver nutrients to the plants. Although the effects of microgravity cannot be simulated on earth, the design is expected to perform better in microgravity. With further testing and refinement, the Accordion can be adapted for a long-term space mission.

INTRODUCTION

From Isaac Asimov to Neil Armstrong, from Christa MacAuliffe to Gene Roddenberry, the dream of visiting other planets and beyond has been imprinted on our culture. Although that dream is not a likely reality anytime soon, the ability to do so is not quite so far away. The technology to send an astronaut to Mars exists, but the ability to efficiently keep the astronauts alive remains to be developed.

The Controlled Ecological Life Support System (CELSS) project underway at NASA is researching the possibilities for providing the astronauts with enough food, water, and oxygen by growing plants in outer space. With the help of the University Space Research Association (USRA), undergraduate design classes have been designing components for use in a CELSS.

With space and mass at a premium, a Variable Geometry Plant Growth Unit (VGPGU) will maximize plant output in a microgravity environment. Though research is scarce in space-oriented versions of a VGPGU, the need for one is fast approaching.

WHY A VGPGU?

In a spacecraft, the environment available to the astronaut has an extremely small volume. Therefore, making the most of the available space is absolutely necessary. A unit that can change volume -- whether it grows plants, holds water, or stores oats -- becomes immensely valuable in such a small place.

Launching a mass out of Earth's gravity well is still a costly venture. Thus, the resources required for a massive device could outweigh the advantages the extra materials may produce. Therefore, low mass designs are attractive.

CURRENT RESEARCH

From the greenhouse to the space shuttle, controlled environments for growing plants have been extensively studied. However, research in variable geometry systems for plants has not

been extensive. Ralph Prince, of NASA/KSC, has done a large amount of work in this area. He has intensively explored how plant spacing affects lettuce growth. (Prince, "Lettuce Production") As Prince discovered in his studies, however, "Of the many systems examined, reviewed in the U.S. Patent Office and studied in scientific literature, only two basic systems are in use. These are the tray and the trough (gully) or pipe systems." (Prince, "Lettuce Production") As guidelines, these designs are ideal because of their extensive use. However, for a microgravity environment neither one is practical due to their mass and free liquids.

The EPCOT Center at Walt Disney World also researches controlled environments for growing plants in The Land. Current research involves numerous nutrient delivery systems and a variety of plants from all types of climates. Many new ideas and concepts were revealed upon one visit, and the impact on this project was substantial.

NASA, of course, is extremely interested in a self-sustaining life-support system for use in outer space. With the future promising extended periods of time in space -- even a trip to another planet -- preparation must be made today.

CHARACTERISTICS

Ideally, a variable geometry unit of any sort should save space. A curious question arises, though: Is space being conserved? The space into which the unit will expand must still remain clear of objects. Temporary storage is possible, but the space cannot be used for any permanent structures. Still, temporary storage is quite an advantage in a small living space.

The mass of a VGPGU will likely be the limiting factor in its microgravity use. The cost of building one could easily be dwarfed by the price of launching one. A low mass, highly effective system would be the perfect solution in terms of mass.

A VGPGU needs to be automatic and easily used so that no time is wasted by the astronauts. Too many other experiments and tasks require attention.

The lifetime of a plant growth unit should be at least as long as the lifetime of its environment. A manned mission to Mars would likely last at least two years, so the unit must have a lifetime at least as long.

Although Prince has concluded that it is impossible to create a universal variable growth unit (Prince, 1992), striving for a widely versatile unit remains a top consideration. If more different types of plants can be grown by one type of unit, then mass production could greatly decrease cost. Commercial might then even become a consideration.

Above all, though, the type of unit for use in space must be usable in a microgravity environment. Water distribution, especially, will be tough to design into a weight-less system because of the behavior of liquids in microgravity. No amount of leaking can be allowed. Also, the behavior of plants in weightlessness is not well known.

All these considerations are important in the design of a true Variable Geometry Plant Growth Unit. It is now time to look at what can be done to meet these specifications.

POSSIBLE DESIGNS

Criss-Cross

Imagine the way cartoon characters would put a boxing glove on the end of a criss-crossing set of wooden bars. They would then lever the other end of the device resulting in a quick expansion of the device -- thereby knocking another character senseless. The initial design developed used that same expanding device without the glove. Instead, at each joint grew a plant in a bulb where the nutrients were delivered.

(Figure 1) The system is simple in design, but it still has many moving parts. Also, maintenance would require that each bulb be cleaned and checked. However, a computer could very easily handle the expansion of the system without human help. The criss-cross design was quickly abandoned for its complexity and maintenance.



Figure 1: Criss-Cross Design

The Telescope

Another candidate was based on the classic telescope. (Figure 2) The expansion of the system was allowed by the concentric pipes from which the plants grew. This system, linear in nature, combined the nutrient delivery system inside the tubes that cause the expansion. The plants' roots grew into the tube as the leaves grew outward. Maintenance would be reasonable, but several other problems remained. In order to slide, the pipes must have openings through which to move. Leakage and corrosion could result.

The Tracked Wheel and The Wedge

An entirely different approach to the problem brought up two new ideas. The previous systems required that plants be planted and harvested all at the same time. This time, a system for continuous use was considered. In the tracked wheel, the plants are initially in the center of the wheel and move radially outward as they grow taller and wider. (Figure 3) The wedge contains new plants in its narrow end which move on tracks to the wide end as they grow. (Figure 4) Essentially, the wheel and the wedge are the same design in different shapes.

Problems with this unit were similar to the telescoping unit. The tracks must move yet create a watertight seal. Leakage is quite possible as is corrosion. Also, the mass of the unit would be the largest of the designs in

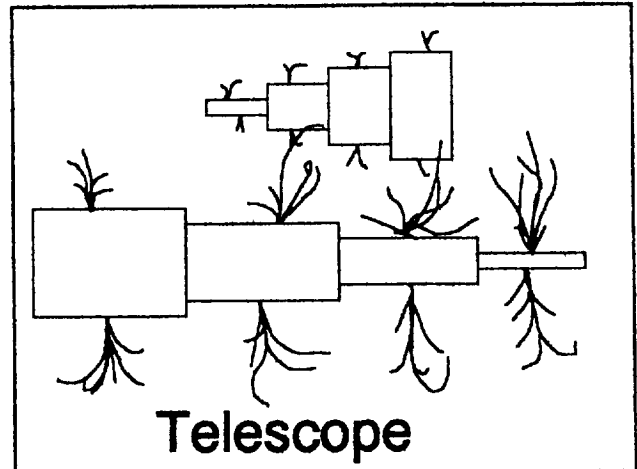


Figure 2: Telescoping Tubes

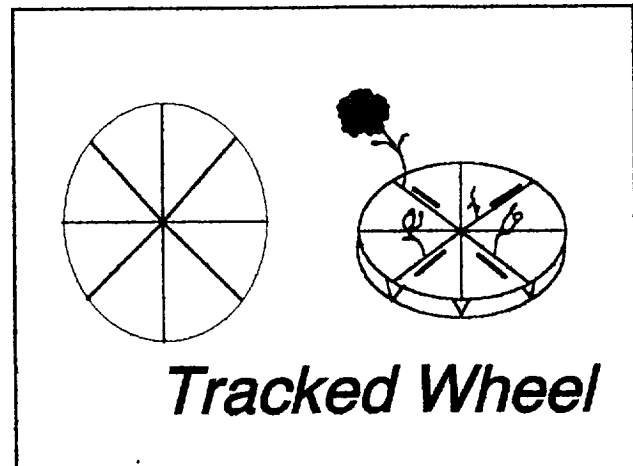


Figure 3: Tracked Wheel

consideration. Maintenance could be time consuming and access to the unit would not be easy. The complexity of the tracked wheel and the wedge create many problems for space-oriented use.

The advantages of these designs, though, are intriguing. Continuous harvesting would contribute to a set routine as well as providing a constant source of food. The system is not truly variable in geometry, though, for the device itself does not change. In fact, a viable nutrient delivery system for these designs has already been researched by former undergraduate students in this program. (Hessel, "Aeroponic") Even after considering the disadvantages, these designs remain viable.

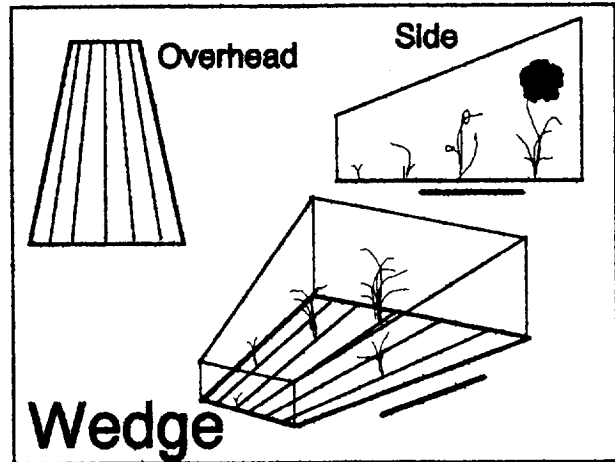


Figure 4: The Wedge

The Accordion

The final design considered resembled an air-duct pipe. The accordion design is a pair of concentric, flexible, expandable tubes. (Figure 5) The plants grow radially outward from the outer tube. The inner tube delivers the nutrient solution and the space between the two tubes connects to a vacuum to suck out the nutrient solution before it can leak out.

This is by far the simplest design of those considered. The mass need not be high since the tubes could be made of a light polymer. Maintenance could be as simple as blasting water through the fully-extended tubes. The tubes could be arranged radially from a common point, concentrically around each other, or even just row-by-row. The versatility of this design is quite high.

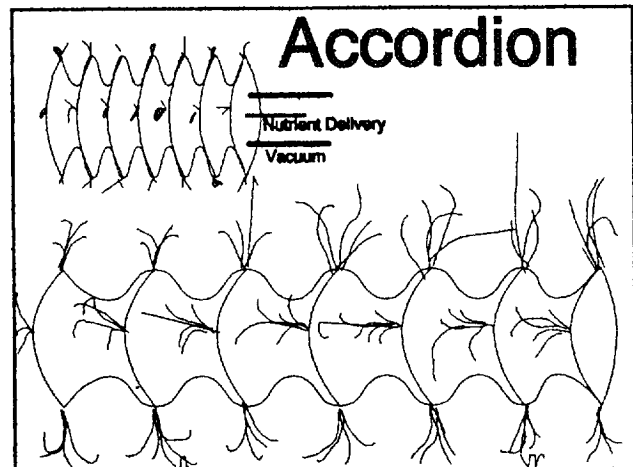


Figure 5: The Accordion

The biggest drawback remains the behavior of liquids in microgravity. The nutrient solution may be moved by the flowing air, or it may stick to the tube surfaces instead. However, the plants can grow radially along all parts of the tube. Still, until liquids are understood, any earth-bound system will have problems.

DESIGN CHOICE

After the strengths and weaknesses of each design were evaluated, no design was clearly the best. However, with the restrictions of time and budget, the Accordion design was selected as the most promising. The largest drawback on the other designs was their complexity. Many moving parts can create havoc when only one fails. The Accordion has no parts that are in continuous motion. This simplicity will result in a remarkable decrease in the problems the VGPGU will have to solve.

FABRICATION

Prototype

The original design of the Accordion was simple enough to provide a quick and easy prototype to be built. Created by slices of PVC pipe connected by dryer hose, this design was the initial testing device. The plants grew through holes cut in the PVC slices. Everything was connected through standard silicone caulking. The prototype's durability was never an issue since it was only intended to last long enough to conduct tests on the plants and the design. As an information-gathering device, the prototype Accordion smoothed the way for a more sophisticated version.

Second Wind

The second version was cut from a clear plastic acrylic pipe instead of the PVC pipe used in the first prototype. In reality, a transparent system would create a lot of algae growth, but for testing purposes, seeing the inside of the VGPGU became important. The second system had only one row of holes -- one per plastic slice. Plants can then be grown in normal gravity as a control for the first prototype.

The Details

Plant support. With a place to hold the plants, a way to hold the plants became necessary. Sponges and peat moss seemed impractical because of future breakdown and rotting. The Land at EPCOT Center in Disney World uses rock wool, rock spun like cotton, for most hydroponic systems. However, local vendors did not have any rock wool available. A past student, however, invented a similar system and used neoprene to hold his plants. Test results showed neoprene to be supportive and non-toxic.

Nutrient Delivery. Nutrient delivery was never intended to be a large part of the VGPGU project. However, some sort of system is necessary for testing, and any practical version requires such a system. The system used contained a three-phase pump and a delivery tube. A timer and relay controlled the time that the pump was running. Constant nutrient delivery is not necessary for plants to grow.

Originally a concentric second tube was to run inside the first one. However, the discovery of helical tubing similar to a telephone cord resulted in a new idea: The tubing was simply poked with holes, and as water ran through the tube, the resulting water spray was more than adequate for the plants. There are drawbacks; for instance, the water spray occurs everywhere rather than concentrated on the plants. Also, as the cord-tube is expanded, it changes shape and the water holes change angle. Still, the results are very promising.

Nutrient removal. With nutrient delivery now possible, some sort of water removal is necessary. For testing, simply using gravity is possible, but then the effects of microgravity may ruin the design later. Research provided information on airflow removal of the liquid nutrients, however the cross-sectional area of the tube proved too large for a simple vacuum on one end of the tube. Therefore, on the other end of the tube a fan was connected. The air-flow prevents water from attaching itself to sides or plants before being directed out of the tube and into the vacuum.

EXPERIMENTATION

Plants

Due to the time constraints of the project, quick growing plants were needed. The best available plants with short growth times were lettuce and spinach. Early in the project, these plants were started conventionally to see how quickly they would grow and how well they would respond to artificial lighting.

Unfortunately, none of these plants were as fast-growing as expected. Other strains being investigated at EPCOT Center were suggested; these new strains became the eventual test plants.

Prototype

The quick design of the prototype allowed certain feasibility tests to be performed. The results helped modify and adapt the second VGPGU for full-scale use.

Plant affinity. Small pieces of neoprene were pierced with holes in which plant seeds were inserted. For a period of a week, these seeds were left in water to test their ability to germinate. Some of the neoprene was inserted into grommets similar to the ones inserted in the VGPGU holes; some neoprene was left floating freely. In addition, two sections of peat moss with seeds were placed in the water.

The results were only partially successful. The seeds did manage to germinate, however they did so rather slowly. A seed that managed to fall out of its own piece of neoprene germinated better than any of the others. The peat moss soaked up a lot of water and crumbled; in microgravity, this could mean particles floating everywhere, so peat moss was quickly abandoned as an option. The final decision was to go with neoprene and grommets holding the plants.

Mechanical Ability. The VGPGU held up under its own weight in many different orientations, and it also showed a lot of flexibility. In the second VGPGU, the lengths were carefully measured to make the maximum use of the volume compared to the expected growth of the plants.

Water tight. The prototype proved to be watertight as hoped. The caulk easily sealed the plastic tubing and the PVC slices. In the second accordion, clear plastic slices and clear caulk were used with the same results.

Easy implementation. The accordion proved extremely easy to move and manipulate. Operator access was simple. In order to simplify testing, the second VGPGU was designed with the holes for the plants in a single row, however the prototype's multiple holes also showed a lot of versatility for microgravity applications.

Location and Environment. The VGPGU was tested inside a small one-room building with no air-conditioning or other environmental controls. Since no windows were in this room, the only light available to the plants was from the fluorescent lights provided for the unit.

Noise was the largest factor at this location. The pump and vacuum created a large amount of noise during operation. In addition, the room contained air-compressing equipment that occasionally added to the noise level. Even though the noise would not affect the VGPGU itself, the plants could be influenced.

Results

The VGPGU succeeded at holding, feeding, and watering the plants. The experiments run indicated our water pressure and airflow were too high. Air pressure too high caused the plants to be blown out of the apparatus; too much water created a lot of leaking through the simple caulked seals of the prototype. However, the results were encouraging. The plants did manage to survive within the Accordion and further experiments can help determine optimal airflow and waterflow.

The system as a whole proved successful at its intended purpose. Microgravity tests would need to be made, but the Accordion proved to be effective and efficient for both time and space.

CONCLUSIONS

The Accordion succeeded at many difficult problems associated with growing plants in microgravity. Most notably, the nutrient delivery system managed to water the plants adequately without causing leakage to the outside environment through the seals around the plants. The nutrient removal contained the water using the air flow. Gravity prevented a fair test of the nutrient removal system, however the airborne water particles moved through the system as designed.

The VGPGU also adapted to different shapes to allow for different size plant spacings. Individual partitions of the VGPGU were able to change independent of the rest, and in addition, the system is also able to twist into a circular shape and expand radially instead of linearly. The geometry proved to be very versatile and adaptable.

Finally, the plants were able to live inside the VGPGU. Should growth and harvest be possible, the Accordion would make a suitable design for a long-term manned space mission. The ability to recycle waste products and oxygen allows astronauts to survive for extended periods of time. Thus, the restrictions placed on human exploration of space ease, and the realm that has caught the dreams of millions shall become the reality of a new generation.

WORKS CITED

Downs, R. I. and Hellmers, H. *Environment and the Experimental Control of Plant Growth*. Academic Press. London, 1975.

Hessel, M. I.; Richert, G. E.; and Nevill, G. E. "Airflow-Contained Aeroponic Nutrient Delivery for a Microgravity Plant Growth Unit." (Publication pending.)

Prince, R. Personal Contact. NASA CELSS. December 22, 1992.

Schwarz, M. *Guide to Commercial Hydroponics*. Isreal Universities Press, 1968.

Mass Determination Device

**Jeff Burke
Mark Cates
Tom Rossi
Jeff Yang**

Table of Contents

SUMMARY.....	30
INTRODUCTION	31
BACKGROUND INFORMATION.....	31
Acoustical Acceleration	32
Dynamic Spring -Mass.....	32
Fluidic Pressure Sensing.....	33
PRELIMINARY DESIGNS.....	33
Bearing Method.....	34
Joint Method.....	35
Spring Scale Method.....	36
Strain Gage Method.....	36
Hall Effect Method.....	37
THEORY OF OPERATION (MDD).....	38
HARDWARE DESCRIPTION	38
Variable-Speed Motor.....	38
Frame and Shaft Assembly.....	39
Arm Assembly	39
Tray Assembly.....	40
Instrumentation.....	40
DISCUSSION OF RESULTS	42
Interpolation Method.....	44
Accuracy	44
Changes and Improvements.....	45
CONCLUSION.....	46
WORKS CITED	47

SUMMARY

The determination of mass in microgravity is essential for scientific research. The Mass Determination Device (MDD) group developed an instrument that utilizes centripetal force to determine the mass of solids (granular and compacted), liquids, and suspensions in microgravity. Currently, instrument's do not exist that possess this much versatility or employ the novel approach of centripetal force to determine mass. The device consists of a frame, motor, controller, transducer, and tray (for holding the mass). The transducer selected for this project applied the Hall Effect to measure displacements resulting from centripetal acceleration.

INTRODUCTION

The determination of small masses (1 to 500 grams) in microgravity is essential for scientific research in space. The mass determination methods currently used for solids and fluids have limitations. For mass measurements, a vibrating system is frequently utilized. This system may be inappropriate depending on the medium being measured. For example, the mass measurement of fluids has typically been plagued by sloshing from surface waves. This problem has resulted in the need for tedious fluid handling techniques to reduce the amount of air in containers of liquids.

The goal of this group was to design a device that accurately measured both solids and liquids. To achieve this versatility the concept of centripetal acceleration was incorporated into the design. This concept was an important step in the development of the MDD, a working mechanism capable of measuring the mass of solids (granular and compacted) and liquids (homogeneous, heterogeneous and multiphase solutions). In addition, the MDD has few restrictions on the container for the mass being measured.

Topics discussed in this paper:

- Current Methods
- Preliminary Designs
- Fabrication of MDD
- MDD Instrumentation
- Future Recommendations

BACKGROUND INFORMATION

The National Aeronautics and Space Administration (NASA) has flown a number of dedicated life sciences missions involving mass measurement technology. These missions along with NASA research centers and other institutions have primarily tested the following methods for measuring mass: acoustical, dynamic spring-mass, and pressure sensing techniques.

Acoustical Acceleration

The Jet Propulsion Laboratory (JPL) is developing an acoustical method for the measurement of mass. This project focuses on accelerating an unknown mass in a microgravity environment using a sound wave generated pressure field. By measuring the field strength, the displacement of the mass and the time to translate the distance the unknown mass is calculated. The advantage of this method is that the mass of small solids and liquids can be determined accurately without a holding container. The main disadvantage of the acoustical method is its limitations on the size of the sample. The method is predominately for droplets of liquids and solids weighing under one gram.

Dynamic Spring -Mass

The Southwest Research Institute has developed the Small Mass Measurement Instrument (SMMI) for NASA, which flew aboard the space shuttle Columbia in June 1991. The SMMI is a spring-mass oscillating system that undergoes simple harmonic motion. If an object whose mass is m and the tare mass m_t are offset from their equilibrium position and released, they will oscillate at the natural frequency f of the system (Solberg, 1991). Using Newton's second law of motion and classical mechanics, the natural frequency of the oscillation is of the form,

$$f = \frac{1}{2\pi} \sqrt{\frac{k}{m+m_t}}$$

where k is the spring constant. Now by substituting the period of oscillation T for the reciprocal of the natural frequency and rearranging the equation,

$$m = k \left(\frac{T}{2\pi} \right)^2 - m_t.$$

The mass of an unknown object can be determined.

The SMMI can determine the mass of solids over the range of 0.1 to 10,000 grams with an accuracy of 2.5%. Because the SMMI is a single degree of freedom spring-mass

system, its major problems are with vibration transmission and a tendency to slosh free boundary fluids.

Fluidic Pressure Sensing

The mass of a homogeneous (constant density) fluid is acquired by rotating the fluid at a constant speed with measurements obtained of the pressure and the angular speed. Using Bernoulli's equation for a steadily rotating rigid continuum,

$$P(r) = P(0) - \frac{1}{2} \rho \omega^2 r^2$$

where $P(r)$ is the pressure at a distance r from the axis of rotation, ρ is the density and $P(0)$ is the fluid pressure at the center of rotation. Knowing the fluid volume V and solving the equation for ρ , then

$$m = \frac{2V(P(0) - P(r))}{\omega^2 r^2}.$$

This method has several obvious limitations. It is not effective for solids or heterogeneous fluids. Also, pressure measurements must be made at two different radial locations.

PRELIMINARY DESIGNS

The conceptual stage of the design process generated numerous ideas for a mass determination device capable of performing in microgravity. The first design decision was to utilize centripetal acceleration. From this decision various techniques for the actual mass calculations evolved. Five preliminary designs for a mass measurement device are listed below:

- Bearing Method
- Joint Method
- Scale Method

- Strain Gage Method
- Hall Effect Method

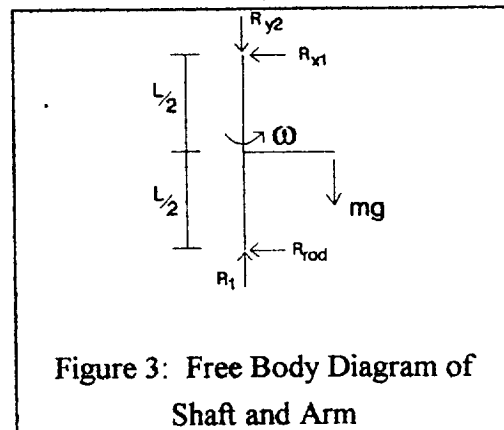
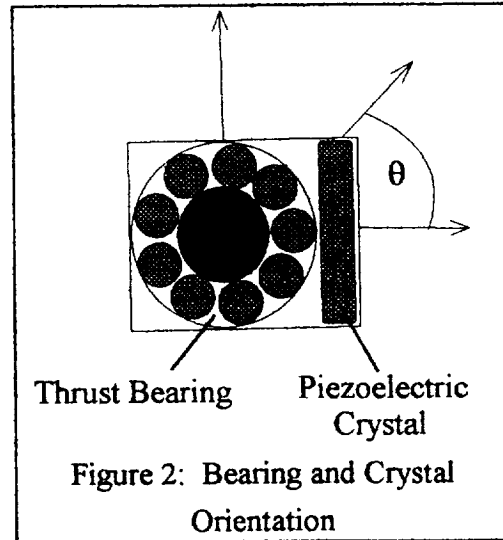
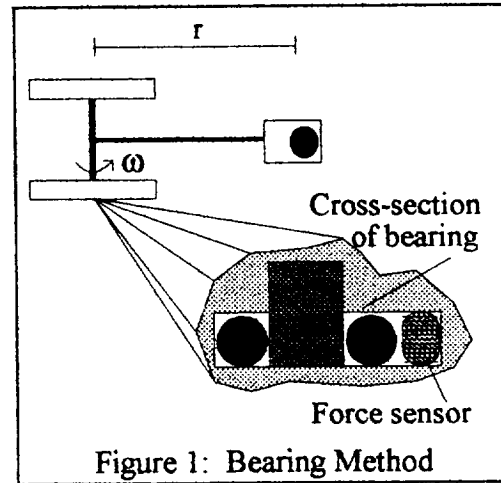
Bearing Method

In Figure 1, a simplified view of the MDD implemented with a piezoelectric crystal as the force sensor can be seen. The bearings are enclosed so that minimal motion takes place in the direction of the thrust bearing. When $\theta = 0^\circ$ for the accelerated mass, the crystal is expected to supply the entire reaction force to the shaft. Assuming the surface between the bearing and base is frictionless, or the friction is accurately measured, the crystal will provide a periodic voltage, whose peak corresponds to the maximum force transmitted by the shaft. Figure 2 shows a detailed view of the crystal's integration into the bearing setup.

A simple point-mass model of the accelerated system is developed accounting for the weight of the mass, the centripetal acceleration, and by assuming the shaft and arm are rigid and weightless. Figure 3 shows the external forces acting on the accelerated system, along with a free body diagram of the shaft. The resulting equation from the free body diagram is,

$$m = \frac{2R_{rod}}{r} \left(\omega^2 + \frac{2g}{L} \right),$$

where R_{rod} is the force measured by the crystal, L is the length of the shaft and g is gravity. The



advantages and disadvantages of the bearing method can be seen Table 1.

Table 1 Bearing Method	
Advantages	Disadvantages
1. Piezoelectric crystal technology exists 2. Simple design 3. Easy to transmit data from bearing to ground	1. Friction may cause errors in force measurement

Joint Method

As can be seen in Figure 4 the joint method is implemented using a T-shaped connection. The T-shaped coupling is connected to the arm rigidly, which is attached to the shaft. When the shaft rotates, the T-shaped arm moves outward pressing on two force sensors. Each force sensor is located between the T-shaped coupling and the arm attached to the shaft. The force detected by the sensors will equal the centripetal force acting on the mass. The resultant equation for the mass is as follows:

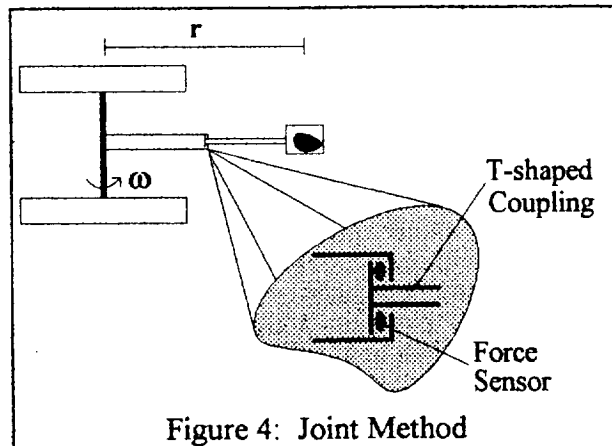


Figure 4: Joint Method

$$m = \frac{F_1 + F_2}{\omega^2 r}$$

where $F_1 + F_2$ are the sum of the forces sensed by the crystals and r is the distance to the center of mass. The advantages and disadvantages of the joint method can be seen Table 2.

Table 2 Joint Method	
Advantages	Disadvantages
1. Piezoelectric crystal technology exists 2. Simple design	1. Arm may not remain perpendicular to gravity field for earth-based testing 2. Frictional errors at joint 3. Transmit data from rotating shaft

Spring Scale Method

This method involves the modification of an existing force-measuring scale. The spring scale is rigidly attached at the end of the arm. The scale's measuring surface would point directly at the rotating shaft, allowing measurement of radial forces. The mass would then be placed inside a container on the scale as shown in Figure 5. The shaft would then be accelerated to terminal angular speed. The centripetal force would push the mass onto the scale's measuring surface with a force proportional to its mass.

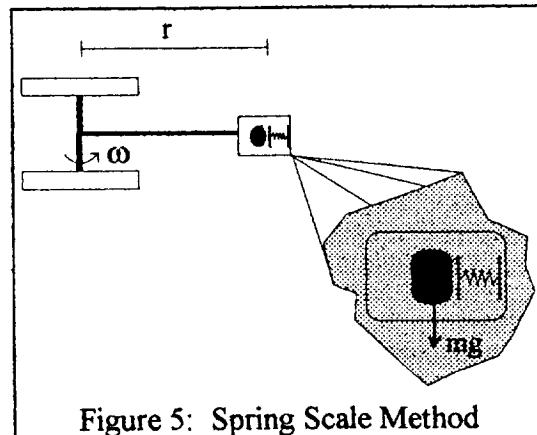


Figure 5: Spring Scale Method

Table 3 Spring Scale Method	
Advantages	Disadvantages
1. Accurate scale technology is available 2. Simple design	1. Transmit data from a rotating shaft 2. On earth, friction may cause errors

Strain Gage Method

This method uses an electrical resistance strain gage to ensure accurate measurements of normal strains. This design is shown in Figure 6. The strain gage is

epoxied to the spinning arm. As the arm is strained the electrical resistance of the gage is changed. This change in resistance is measured and then calibrated to directly read strain, ϵ . From the measured strain we can calculate the mass by using stress-strain and centripetal force relationships. The resulting equation is,

$$m = \frac{E\epsilon}{r \left(\frac{w^2}{A} + \frac{gy}{I} \right)},$$

where E is Young's modulus, A is the cross sectional area of the arm, and I is the moment of inertia. The value y is the distance from the centroid of the arm's cross section to the furthest point on the cross section. The advantages and disadvantages of the strain gage method can be seen in Table 4.

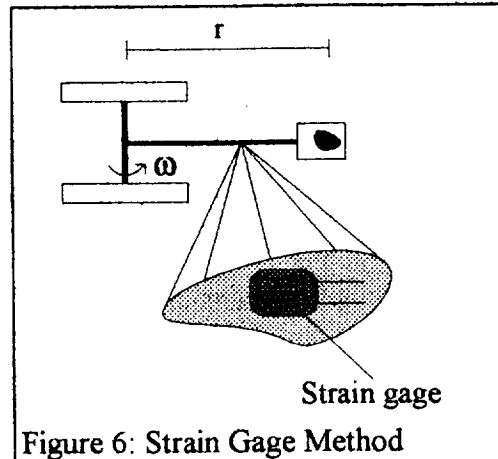


Table 4 Strain Gage Method	
Advantages	Disadvantages
1. Strain gage technology already exists. 2. Simple design.	1. Transmit data from rotating shaft to ground. 2. Signal is typically small.

Hall Effect Method

This method was the final choice for implementing the MDD. In general it uses a Linear Output Hall Effect Transducer (LOHET) to sense radial changes in distance of a centripetally accelerated mass.

The mass is placed at the end of a rotating arm on a leaflet spring tray. As the arm is rotated the inertia of the mass will cause the tray to defect radially outwards. By placing magnets on the tray, the LOHET can sense the displacement of the mass. The deflection is given by,

$$\Delta x = \frac{m \omega^2 r}{k}$$

The relationship between the LOHET's signal and Δx is not readily predictable. Because of this, the LOHET device must be carefully calibrated. This was done by creating several constant frequency calibration plots over a range of masses. From these plots the MDD is capable of making actual mass measurements.

Table 5 Hall Effect Method	
Advantages	Disadvantages
<ol style="list-style-type: none"> 1. LOHET technology already exists. 2. LOHET can be oriented in numerous directions to increase signal range and strength. 3. High signal strength. 4. Small size. 	<ol style="list-style-type: none"> 1. Data must be transmitted from the rotating arm to ground. 2. Must be calibrated completely.

THEORY OF OPERATION (MDD)

As explained previously in the Hall effect method section, the MDD will operate by measuring the deflection of a centripetally accelerated mass. The mass will be attached to a spring tray at the end of a rotating arm. By spinning the arm at a constant speed the mass of the object will be obtained.

HARDWARE DESCRIPTION

Variable-Speed Motor

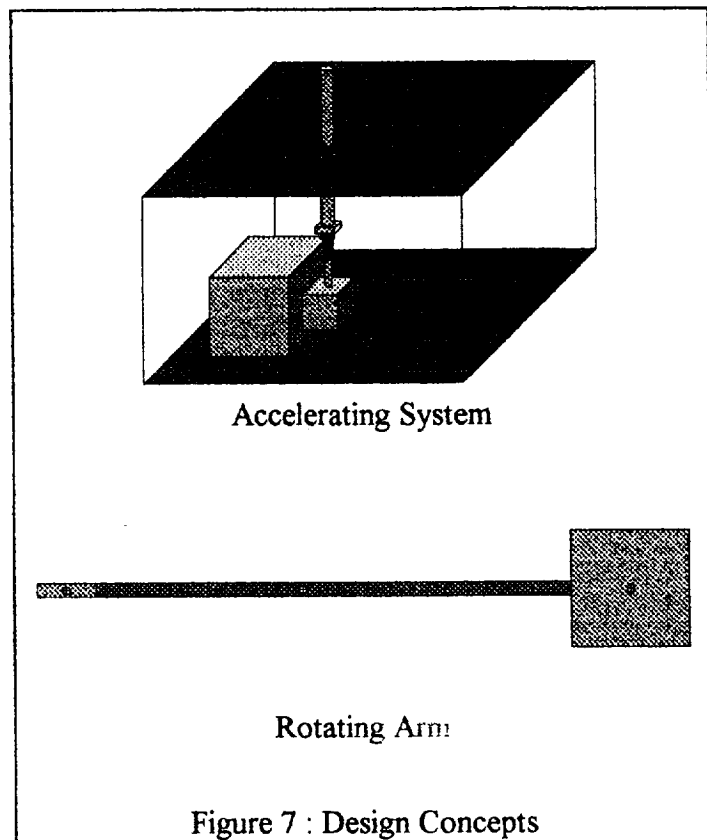
A variable-speed DC motor was obtained from General Controls, Inc. This DC motor has two major elements. The armature is the rotating element of the motor. The armature rotates at speeds that are proportional to the DC voltage applied across the two armature terminals. The other major element is the field. The field is the stationary

element of a DC motor and it provides a magnetic flux with proper polarity to cause the armature to move when armature voltage is present.

The variable-speed motor was used in order to preserve flexibility in the MDD. Since, this type of motor maintains a constant torque the speed range can be varied. This would allow testing of the same load or mass at different speeds without concern to the motor's performance. The dimensions for the motor can be seen in the Appendix.

Frame and Shaft Assembly

To reach the goals of the MDD group a structure that would provide stability for the entire system needed to be designed and fabricated. The design concept is shown in Figure 7. This structure was effective, yet simple in design and fabrication. The structure was constructed of steel side-angles and two aluminum plates. The aluminum plates support the shaft used to accelerate the arm of the system. The arm is mounted at the top of the shaft. A flexible couple is used to connect the shaft to the motor.



Arm Assembly

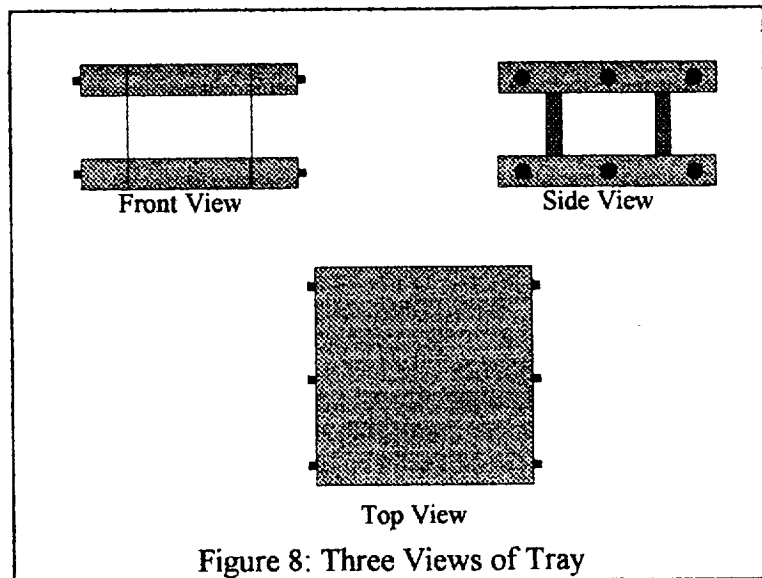
A flexible couple is used to connect the arm to the shaft. The power source (14 1.5V AA cells) for the instrumentation is located on the arm and also functions as a counterbalance for the entire system. Located at the opposite end of the arm is the spring-tray mechanism used for holding the unknown mass.

Tray Assembly

The tray consists of two aluminum plates that firmly hold the four strips of spring steel. Figure 8 shows a close up view of the tray. It should be noted that at the outset of construction, the alignment of the spring steel was thought to be crucial. However, it was found that considerable misalignment could be endured while still obtaining accurate deflection results.

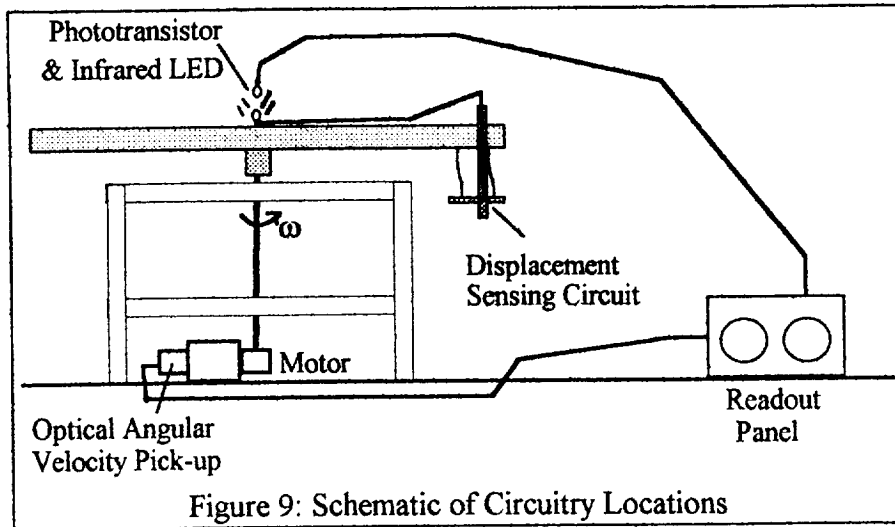
A pair of magnets is attached to the side of the tray. The magnets are placed in this orientation so that the

magnetic field strength would vary almost linearly. This allows the LOHET to measure deflection while attached to the spinning arm.

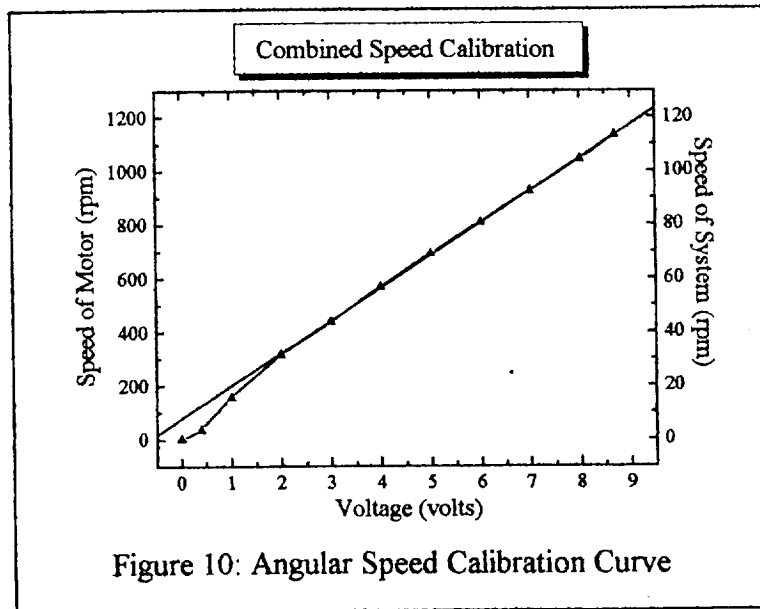


Instrumentation

The major requirements on the instrumentation system are to measure the angular speed of the shaft and the displacement of the mass. In addition to measuring the displacement, the information must also be transmitted from the rotating arm to a stationary readout panel. A schematic of the overall setup is shown in Figure 9.



Angular Speed Measurement. The angular speed of the vertical shaft is difficult to measure directly because of its low rotation speeds (0-2Hz). This is due mainly to fact that most modulation circuitry is expected to operate at frequencies greater than 10-20Hz. This problem was circumvented by measuring the frequency of the motor's armature, which is approximately ten times faster than the vertical shaft. The frequency of the armature was measured by demodulating a pulse train of square waves generated from an optical pick-up inside the motor. The pick-up gave an additional gain by producing 30 square waves per revolution. This amounted in a multiplication of the vertical shaft's low frequency by 300; thus, making the frequency readable by standard demodulation circuits. The demodulation was accomplished through a 4046BE phase-lock loop chip. The calibration curve for the angular speed versus output voltage, V_f is shown in Figure 10.



Calibration of the demodulated output was done by using a pulse counter to measure the exact frequency of the armature. This frequency was then assumed to be 10 times greater than the vertical shaft. This assumption is not exact and a more accurate measurement can be made by using another optical pick-up on the main shaft to determine the exact gear down ratio.

Displacement Measurement. The displacement of the mass was measured using a LOHET from Micro Switch Co. (Part # 91SS12-2 and 2 Indox 1 magnets (0.25" diam. and 0.125" long)). The magnets were placed such that the north and south sides were adjacent allowing the LOHET to slide by both the negative and positive flux poles. This orientation gives flexibility to the LOHET by producing a wider voltage range (1-10VDC) and a larger range of measurable deflections (0-0.5in). It should be noted that the LOHET was also approximately 0.03125" from the magnets. At this gap distance it was noticed that small changes in gap distance (due to vibrations) cause substantial changes in the output voltage (+0.1 VDC) of the LOHET. In retrospect this could be changed by using a more rigid support for the LOHET and more secure fasteners for the spring steel.

Signal Transmission. The voltage from the LOHET was first sent through the voltage controlled oscillator (VCO) on a 4046BE chip. After this modulation, it was then transmitted via an infrared LED across 1cm air gap to a stationary phototransistor pick-up. The signal from the phototransistor was then demodulated (using another 4046BE) to produce an output voltage, V_s . The output was then displayed on a two channel oscilloscope.

DISCUSSION OF RESULTS

With the signals V_s and V_f for the displacement and the angular speed, two single calibration curves were generated for $f = 0.8\text{Hz}$ and $f = 1.78\text{Hz}$.^{*} These plots are presented in Figure 11. Because of the time limitation on the project more calibration curves could not be generated. However, predicted typical plots for a given frequency are also shown in Figure 11. These plots are presented to demonstrate what a complete calibration procedure requires.

^{*} The angular speed of the system can be referenced as a speed or frequency.

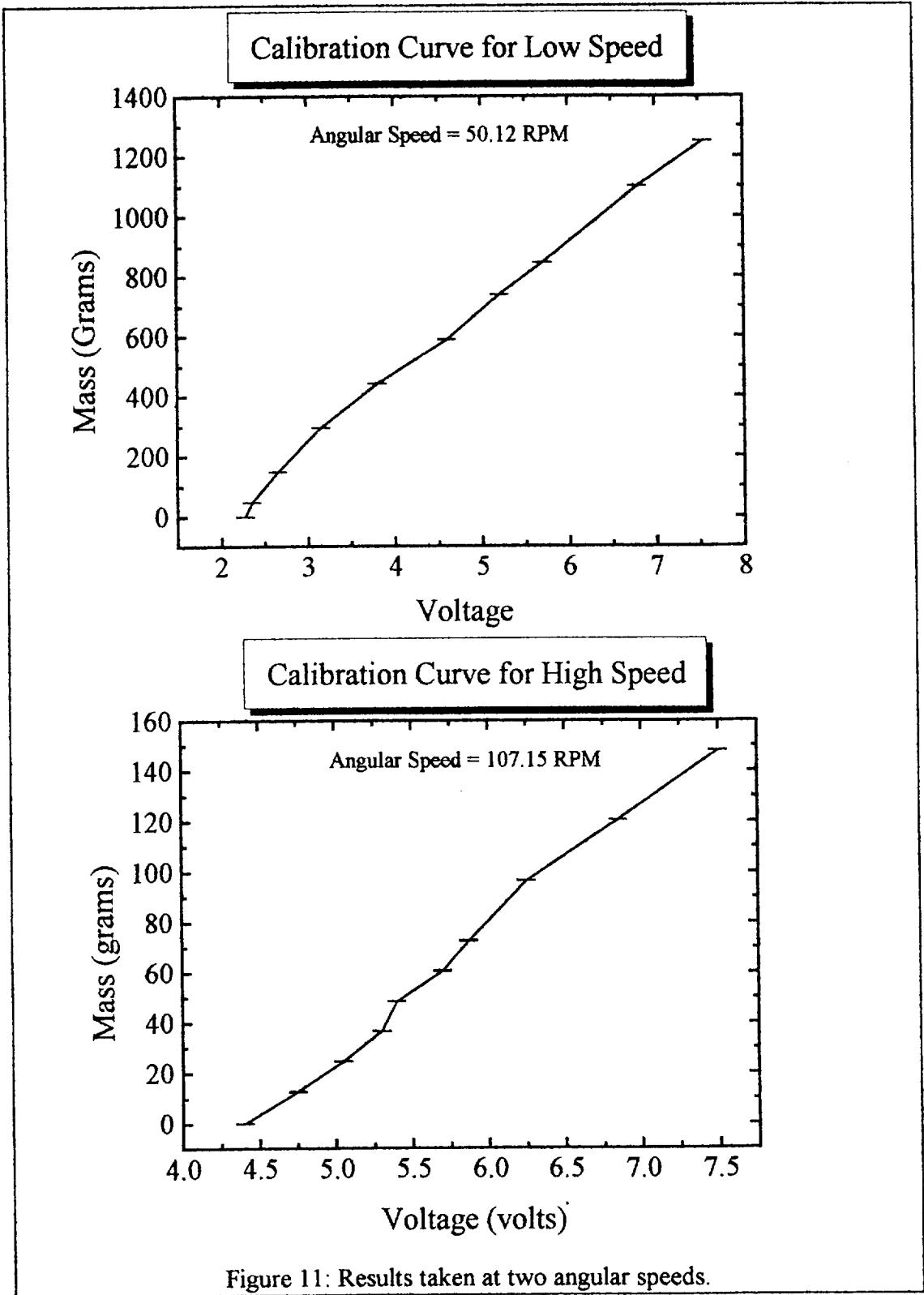


Figure 11: Results taken at two angular speeds.

Interpolation Method

Although the calibration plots are shown for discrete frequencies, it is obviously more preferable to make measurements at any motor speed. An interpolation method is presented here to estimate the mass of a sample at frequencies other than those on the calibration plot. For example, if the measurement was made at $f = f_o$ resulting in the output, $V = \text{const.}$, then the mass would be approximated as,

$$m_{f_o} = \left(\frac{f_o - f_1}{f_2 - f_1} \right) (m_{f_2} - m_{f_1}) + m_{f_1}$$

where f_1 and f_2 are the nearest known frequency calibration lines from Figure 12. The masses m_{f_1} and m_{f_2} are simply the masses at $V = \text{const}$ on the lines f_1 and f_2 .

It should be noted that the interpolation scheme has not been tested. However, the only doubt is whether the interpolation will function better with a linear (as used above) or a quadratic interpolation. The reason for speculating a quadratic interpolation maybe needed is because of the ω^2 term in the Hall effect's deflection equation. Which scheme to use can be determined by plotting more calibration curves, to see what power law relationship works best.

Accuracy

A complete assessment of the MDD's accuracy could not be made because of the lack of calibration curves. However,

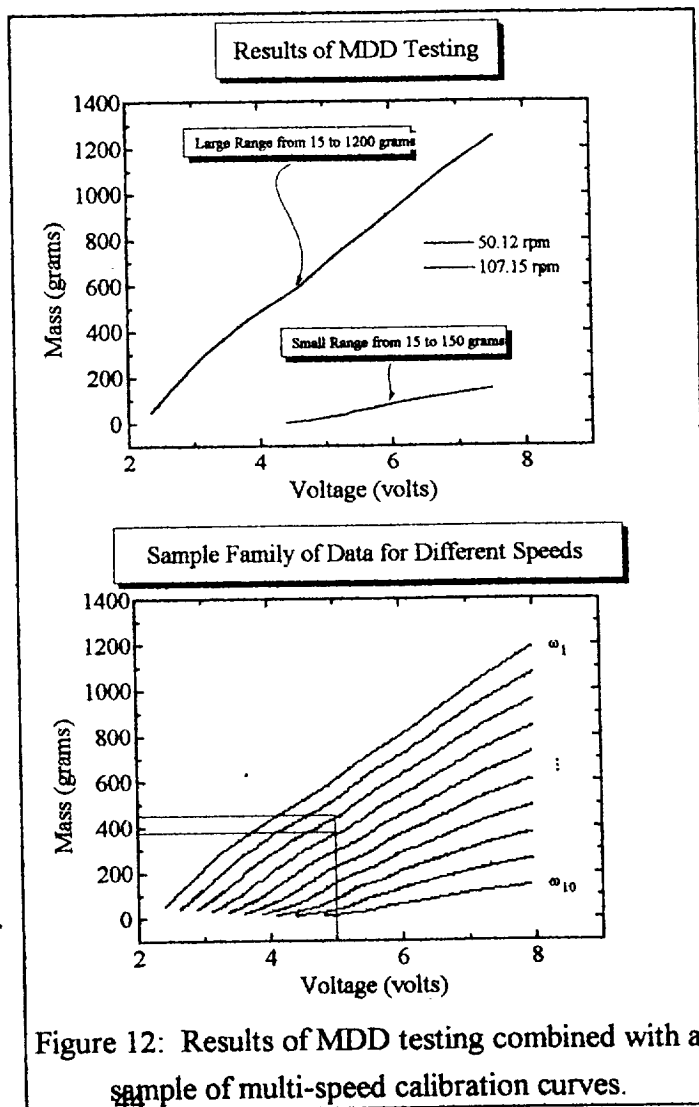


Figure 12: Results of MDD testing combined with a sample of multi-speed calibration curves.

information on the repeatability as well as signal steadiness can be discussed.

Repeatability. The MDD showed a high degree of repeatability for both the angular speed and displacement measurements. This claim is based on almost zero signal drift for a period of 10 hours for the angular speed. The displacement measurement repeatability also seemed rather good---the same measurement ($\pm 0.05\text{VDC}$) was achieved after 10 hours of continual starting and stopping of the shaft.

Signal Steadiness. Of the two signals only the displacement voltage fluctuated noticeably. The steadiness of the displacement signal is controlled by several factors, namely, oscillation of the tray, and sensitivity of the circuitry. The excessive sensitivity of the circuitry was responsible for some of the oscillations. However, some of the signals fluctuated because the mass samples were not lashed down firmly to the tray; thus causing the tray to oscillate perpendicular to the LOHET face. Although this caused substantial fluctuations in the displacement voltage, the signals were sinusoidal and so an average reading was possible. Overall, this probably introduced an uncertainty of about $\pm 0.05\text{VDC}$.

Changes and Improvements

Based on the experience accumulated in constructing and testing the MDD several suggestions can be made for future work.

1. As a matter of practicality the arm will always be imbalanced; therefore, small angular velocities should be used. For the MDD $f < 2\text{Hz}$ worked well.
2. A more rigid restraint for the spring steel and the LOHET should be considered. This will result in a more stable displacement signal.
3. The resolution of analog voltage measurements were also crucial especially for smaller masses where the output signal was rather high (refer to Figure 11 for $f = 1.78\text{ Hz}$). Thus a good resolution for high voltage signals is important.
4. In order to make measurements of small masses ($< 50\text{g}$) it is necessary to spin the device at higher speeds. However, the deflection of the tray for small masses is

mainly dictated by the mass of the tray, and not the mass sample. Therefore, it is essential to reduce the tray's mass for making accurate measurements of small masses. As shown by the $f = 1.78\text{Hz}$ calibration curve the very large angular speed could only produce 4.4 to 7.5VDC for the a mass range of about 0 to 150g. This is about only half the voltage range of the $f = 0.84\text{Hz}$ plot. The range of voltages can be extended to about 2 to 7.5VDC if the tray's mass is lightened. Accomplishing this allows a more accurate measurement of the smaller masses.

CONCLUSION

The MDD illustrated that a rotational device can be used to determine mass in microgravity. The hall effect transducer served as an acceptable mechanism for calculating displacements resulting from centripetal acceleration. A computer can be incorporated into the design to make the MDD easy to use and applicable to everyday scientific research in microgravity.

WORKS CITED

Doddington, Dr. Harold, AeMES Department, University of Florida.

Irwin, D. J. *Engineering Circuit Analysis*. Macmillan Publishing Company. New York, 1989.

Riley, W. F. and Zachary, L. W. *Mechanics of Materials*. John Wiley and Sons. New York, 1989.

Solberg, R. F. "Measurement of Weight in Space." *Technology Today*, 1991.

Wolfson, Richard. *Physics*. Little, Brown and Company. Boston, 1987

Variable Lighting System

**Ed Solozobal
Tu-Ming Leung**

Table Of Contents

INTRODUCTION	50
PRODUCT DESIGN SPECIFICATION	50
BACKGROUND	50
Photosynthesis	51
Energy efficiency	51
Chlorophyll a	51
Chlorophyll b	52
Cartenoids	52
Phytochrome	52
Blue Light Absorbing Pigment	53
Sun and Shade Plants	53
Intensity	54
Various Light Sources	54
Light Emitting Diode	54
DETERMINATION OF THE LIGHT SOURCE	55
Ratio Test	55
Why do LEDs have a Higher Ratio	56
DECISION	58
DEVELOPMENT OF CONCEPTS	58
Concept 1	58
Concept 2	59
Concept 3	59
Final Concept	60
TESTING	60
Results	61
Light Meter Test	61
Power Comparison Test	61
CONCLUSIONS	62
APPENDIX 1	63
WORKS CITED	67

INTRODUCTION

Light is one of the most important factors in a Controlled Ecological Life support system- one that is usually taken for granted. After examining the lighting system at NASA, our group decided that a more efficient design could be developed for plants. Before concepts were developed, an understanding of the light spectrum absorbed by plants was researched. Also, since there were many different light sources available, an efficiency rating was developed in order to choose the most efficient light source. Finally, intensities needed for an average plant were researched to determine which light sources could provide the proper amount of light. Concepts were then developed for the light sources chosen and tests were conducted on them.

PRODUCT DESIGN SPECIFICATION

- Design a light system that uses less power to grow plants.
- Design a light system that is highly efficient so energy is not converted into wasteful heat that must be removed.
- Design a light system that would need less maintenance than a conventional lighting system.

BACKGROUND

In order to decide which light source would be better for a specific plant, we need to take an in depth look at the "light" factors that influence the rate of photosynthesis. These include the light spectrum (wavelength), the effect of light on chlorophyll, the absorption rates, and the light intensity.

Photosynthesis

Photosynthesis is the process to "absorb light energy and convert it into reductive chemical energy" (Attridge, 1). The light requirements for a plant consists primarily of red (R) and blue (B) wavelengths. These waves are absorbed by many different pigments that vary in chemical composition and function. these include the photosynthetic pigments-chlorophyll and carotenoid-and the developmental pigments-phytochrome and BAP (Attridge,

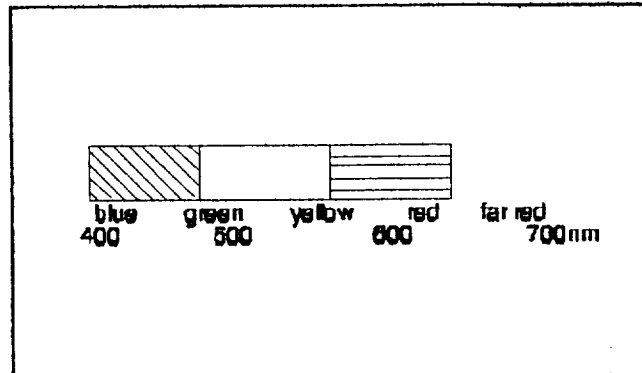


Figure 1. Visible light spectrum.

23). Since these pigments require different wavelengths of light, the absorption rates will be discussed. Light intensity and if the plant is a sun or shade plant are also factors that need to be considered.

Energy efficiency. It should be noted that "regardless of whether the light is red or blue, the same number of einsteins are required for photosynthesis per mole of oxygen formed" (Photosynthesis, 801). The energy equation of an einstein is given by the equation:

$$E=28,000/\lambda$$

where λ is the light wavelength (nm) and E is measured in kilocalories. When light energy is absorbed by a molecule (ie. chloroplast, phytochrome), it excites electrons within that molecule to a higher energy level or excited state. Light of lower wavelengths such as blue (refer to Figure 1) has more energy than light of longer wavelengths such as red, such that blue light creates an excited state of higher energy (Photosynthesis, 803). Therefore, we might logically conclude that blue light would be more efficient for plants. we must remember, however, that some pigments and chlorophyll absorb relatively large amounts of red light.

Chlorophyll a. The most abundant of the photosynthetic pigments, chlorophyll-a (Chl-a), primary function is the conversion of light energy into chemical energy (Note: the conversion process

does not need to be reviewed since all we are concerned with is the spectrum absorbed in order to maximize this process). Chl-a contains two main regions of absorption which is shown in Figure 2. These include one region that peaks at 660nm and the other at 420nm (Attridge, 25).

Chlorophyll b. Higher plants also contain chlorophyll b (Chl-b). Its primary function is the same as Chl-a, however, it is less abundant within the plant structure. Chl-b absorption spectrum is also shown in Figure 2. The absorption peaks at 450nm and 643nm.

Carotenoids. These orange and yellow pigments are also found in higher plants. The most common form is B-carotene. From the absorption spectra (Figure 2) one can see that it is very broad over the blue spectrum peaking three times between 400 and 500nm. This is an advantage to plants since "carotenoids function as accessory pigment for photosynthesis" (Attridge, 24).

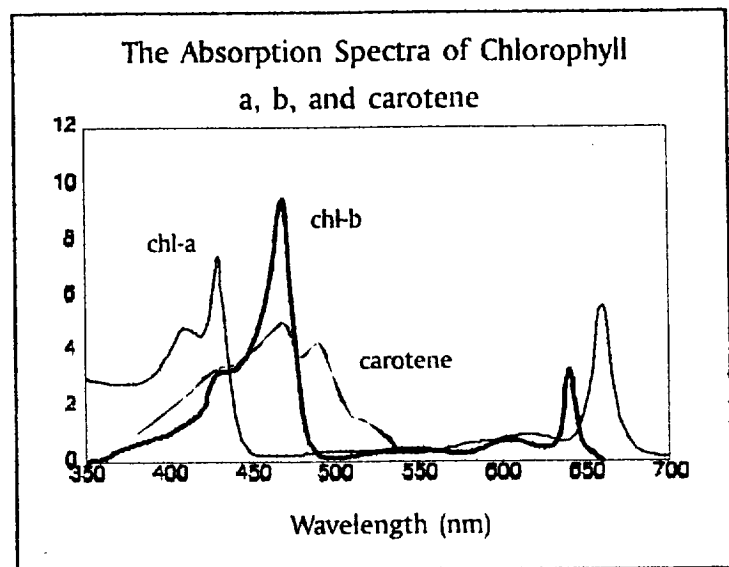
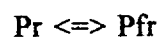


Figure 2. Absorption Spectra of Chlorophyll a, b, and carotene.

Phytochrome. Phytochrome is the best known developmental sensopogment in higher plant life. Phytochrome exists in two forms and the photochemical reaction induced by the absorption of light converts the pigment from one form to the other (Attridge, 25). The two forms known as Pr (red) and Pfr (far red). Their absorption spectra is shown in Figure 3. Phytochrome acts as a "reversible biological switch" as shown in the following equation:



In other words, when Pr absorbs red it is rapidly converted into Pfr which absorbs far-red which is converted back into Pr and so on.

Pfr is believed to be the active form of phytochrome. Under various tests, it was shown that under red light Pfr constituted 80 percent of P_{tot} (Pr + Pfr) (Attridge, 32). However, this leads us to the problem: What happens to the Pfr? Some might be converted back into Pr.

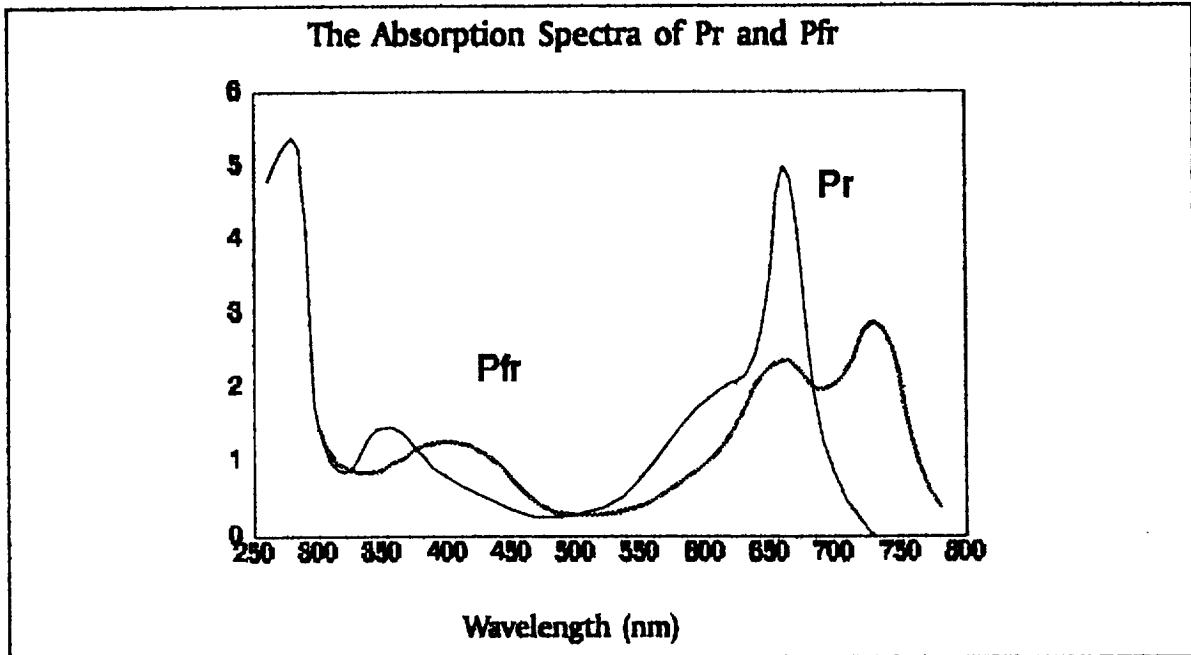


Figure 3. Absorption spectra of Pr and Pfr.

Since Pr and Pfr overlap in this manner, a wavelength with a maximum of 690nm would provide the proper photons for equal absorption by both pigments. Phytochrome's primary function is to accelerate chlorophyll synthesis.

Blue Light Absorbing Pigment (BAP). Due to the fact that most scientists concentrated their efforts into researching phytochrome, they never recognized the possibility that a BAP could exist. Since this recognition has only evolved in recent years, little could be found on the primary function of BAP (or cryptochrome) or its spectra (Attridge, 36-38).

Sun and Shade Plants. Plants need to adapt their photosensitive systems to their environment. Such adaptation can be a long evolutionary process which results in genetically fixed sun and shade plants, or plants can have the flexibility to adapt to intensity and quality of light during development. When exposed to blue light, plants will adapt to sun conditions (higher chl a/b ratio) while under red light they would adapt to shade conditions. Under sun conditions plants tend to grow faster and produce more oxygen.

Intensity

The rate of photosynthesis is dependent on many factors including temperature, carbon dioxide, water, minerals, and light intensity. If all factors are held constant and light intensity is increased, the rate of photosynthesis also increases until a saturation maximum is reached. However, at these extremely high intensities a process known as photorespiration can occur. This process competes with photosynthesis and limits further increases in the rate of photosynthesis. From research we concluded that an average plant needs approximately 1600 lumens/ft². However, this value can change due to the type and size of the plant in question. Andrew Schuerger, senior plant pathologist at The Land, EPCOT Center, suggested that our group use 10 to 20% blue light and 80 to 90% red light in our design.

Various Light Sources

There are many different kinds of light sources that could be used to provide the proper amount of light to a given plant, however, some are more efficient than others. From a lighting study conducted by NASA, our group concluded that four light sources out of 34 were the most power efficient and had the longest lifetime: Standard Gro&Sho (F48T12/1500), High Pressure Sodium (LU1000), Multi-vapor Metal Halide (MVR1000/U), and the LED.

Light Emitting Diode. Luminescence is the result of electronic excitation of a material (Gro&Sho, HPS). The LED is made of semiconducting materials. These materials have a valence and conduction band. Both these bands are separated by an energy gap. The conductivity of the material can be enhanced by introducing impure materials. This is called doping and consists of two types of semiconductors-the p and n-type. The n-type results in additional electrons into the conduction band while the p-type gives rise to electron vacancies or holes that lie close to the energy in the valence band. These two materials are joined by a junction, the excess electrons from the n-type material move to the vacancies in the p-type material and vice-versa. When equilibrium is achieved, a junction potential is created. When a forward-biased (potential) is applied, the potential at the junction is lowered resulting in a

migration of electrons and holes. Charged carriers are injected across the junction converting their excess energy into light (Napier, 20-24).

The photons generated by radiative recombination at the p-n junction are emitted in all directions, but only a small fraction escape from the front surface. The chip is mounted on the top of the cathode inside a reflector dish, which is designed to reduce the loss of radiation due to the critical angle of the emitted light. The anode is connected to the chip by a wire lead. The chip is encapsulated into a plastic cover with a hemispherical lens above the LED junction. The lens is constructed in order to increase the light output from the LED chip by increasing the critical angle.

DETERMINATION OF THE LIGHT SOURCE

Although our group narrowed down the many different types of light sources to four, we needed to narrow them down to one or a combination of two. This was accomplished by devising a rating method which was called the ratio test.

Ratio Test

By using plots of wavelength vs. intensity (refer to Figure 4), we were able to calculate the area under these curves. This area (lumens) was then divided by the amount of power needed to run the light source and to remove any heat produced by that source. Note:

1. The G.E. light sources have a spectrum that contains all wavelengths of visible light -- most of which is not needed by the plant. Therefore, only the areas within 400 to 500nm and 625 to 700nm ranges were used.
2. Originally our group was also going to calculate the power needed to remove heat produced by these sources. The amount of heat generated by a LED is less than any of the other light sources considered, also, the red LED's had higher ratios than the G.E. light sources when the power to produce heat was not incorporated into the ratios. Therefore, the LED's will still have a higher ratio if we did

include power to remove heat.

The results from the ratio test are listed in Table 1. As one can see, the LEDs have a much higher ratio than the other light sources. The blue LEDs, however, do not have a high efficiency like their red counterparts. The miniature blue fluorescent does have a slightly higher ratio.

Spectral Energy Distribution for Different Light Sources

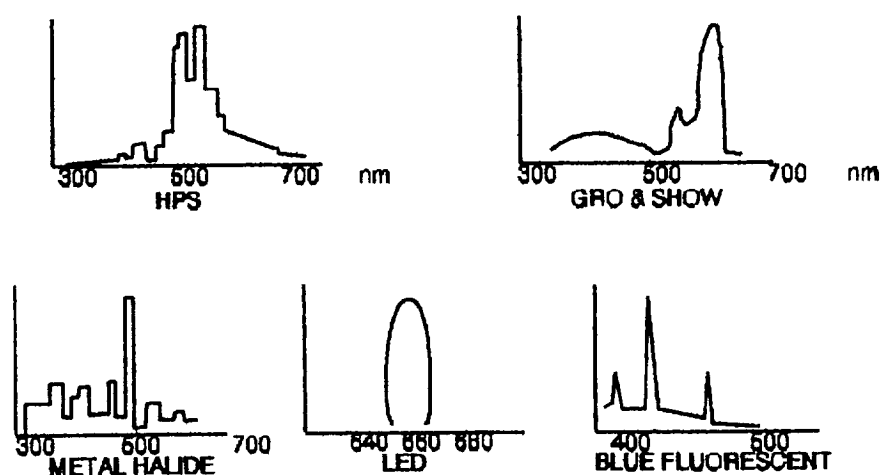


Figure 4. Spectral energy distribution for light sources.

Why do LEDs have a Higher Ratio?

1. LEDs do not produce infrared light waves. This has two benefits: First, no power is wasted in producing these wavelengths, and second, no power is needed to remove the heat generated by infrared light. (Table 2 shows the breakdown of energy for the G.E. light sources).
2. The G.E. light sources contain the complete visible spectrum, however, only 35% of it is used by plants. LEDs, on the other hand, give off a narrow band of visible light. These bands give a closer match to the absorption curves of plants. With

LEDs 85 to 100% of the light generated will be used by the plants.

Table 1. Efficiency Ratios for Different Light Sources

Light Source	Ratio
Gro&Sho	7.5
Metal Halide	38.2
HPS (LU400)	14.5
HPS (LU1000)	17.3
Blue Fluorescent	42
LED (440nm)	47.5
LED (482nm)	22
LED (660nm)	888.2
LED (643nm)	98.2

Table 2. Energy Breakdown in Watts

	Infrared	Visible light	Conducted heat	Ballast loss	Ultra-violet
Gro&Sho	15	10	14	8	.5
Halide	347	228	336	141	33
PS	158	135	90	67	0

DECISION

Our group narrowed down the light sources to two which we used in our design:

1. L200CWR5k red LED (660 nm)
2. BF659-12 miniature blue fluorescent (435 nm)

Our group chose the 660nm LED over the other LEDs because it has a wavelength which matches the absorption curve for chlorophyll-a. As previously discussed, chl-a is the primary photosynthetic pigment. Also, it has the highest efficiency compared with the other LEDs. The blue fluorescent was chosen primarily because the blue LEDs did not produce a high enough intensity for an average plant. Also the blue fluorescent produced a fairly reasonable efficiency ratio in comparison to the other light sources. Figure 5 shows the LED and blue fluorescent curves in combination with the absorption curves. All of the light produced by these light sources is being absorbed by the plants.

DEVELOPMENT OF CONCEPTS

After determining the light sources our group would use, the next step was to develop various concepts which would satisfy our PDS. Four concepts were developed on paper. One was chosen, simplified, and constructed.

Concept 1

In this concept (shown in Appendix 1), the red LEDs are arranged in a circular pattern so different loops can be turned on as the plant grows. The blue light is provided by two fluorescent bulbs located on each side of the top plate. Since these sources emit light in a radial direction, we did not believe there would be a problem with the transfer of blue light to the plants. The top plate will be 17 x 17 cm and the LEDs will be placed 5 mm apart from each other in order to provide the proper intensity level. Since the LEDs have a 8 degree viewing angle, it was calculated that the plate would have to be 2 in. above the leaf canopy in order to

provide a constant intensity.

Spectral Energy Distribution of Blue Miniature Fluorescent and Red LED

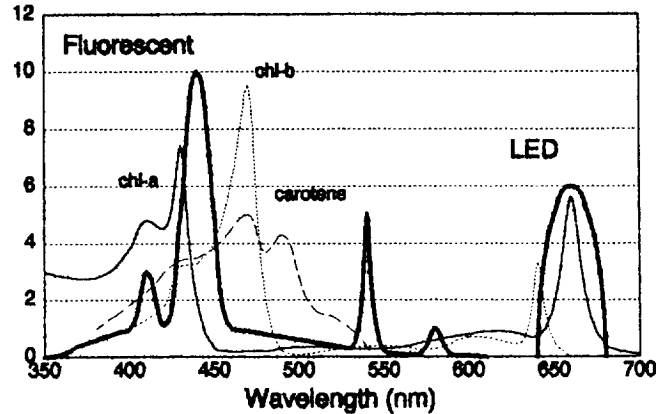


FIGURE 5

The plate can be easily removed for replacement while the fluorescent bulbs can be slipped out from the front since these will be replaced more often.

Concept 2

This concept is much like the first concept with one difference—there is an overlap of LEDs over the canopy of the plant. The reason for this is to provide a larger amount of red light toward the upper sides of the plant since leaves are usually not parallel with the ground. The fluorescent bulbs are still located in the same place and the LEDs on the upper plate are in the same circular fashion (Refer to Appendix 1).

Concept 3

Shown in Appendix 1, this concept compliments the variable plant growth chamber group's project. As one can see, LEDs are placed on an outer cone surrounding the entire growth unit. These will turn on or off at various stages of growth. The blue fluorescent bulbs will be placed as shown, stretching the length of the unit.

Final Concept

This design, shown in Figure 6, is very similar to Concept 2. However, it is circular (20 cm in diameter) in order to mimic the radial plant growth in the horizontal direction. The smaller fluorescent bulbs (50 mm in length) provides us with the opportunity to place them in a circular position so more of the bulb light can be used to illuminate the plant. The overlap consists of three rows of LEDs at a 30 degree angle with the vertical axis. The LEDs are placed 5 mm apart from each other and are attached to a bread board where they are connected in parallel with each other. These boards are placed inside the supporting structure which was made out of aluminum. The fluorescent bulbs are attached

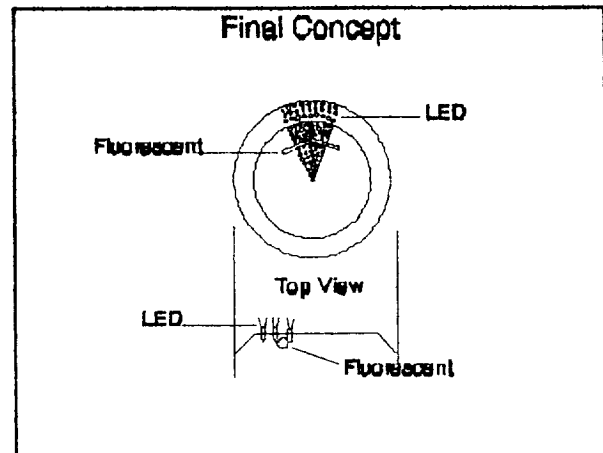


Figure 6. Final concept.

to the underside of this structure. The device is attached to a chemistry test stand which can be adjusted to any height. Eight miniature blue fluorescent bulbs and 529 red LEDs are required for the device. However, because our group was not planning on growing any plants, it was decided to build only 1/8 of the device. Therefore, only 66 LEDs and one fluorescent were required for testing.

The concept is powered by a 12 volt DC power source which is reduced to 2 volts using a voltage regulator for the LEDs. This is in parallel with an inverter which converts the 12 volts into 185 volts and .004 amps in order to operate the fluorescent bulbs.

TESTING

Two methods were developed in order to test our lighting design:

1. A light meter was used to test the relative intensities of light at 7 different areas in the test section and at different heights from 2 to 18 inches (once at every

inch).

2. The power to operate our device was compared to the power to operate the light sources used by NASA.

Results

Light Meter Test. The intensity of the red LEDs remain constant at each different testing area at one height. As we moved the meter away from the LEDs the intensity decreased linearly until we reached 18 inches when the intensity would drop exponentially as we moved farther away. The blue fluorescent produced different intensities in the three regions until we reached the 10 inch mark. The center had the highest intensity in this range because in this area we were testing directly over the fluorescent. When both light sources were turned on at the same time, the results equaled (one percent error) the addition of both source's intensities that were measured separately.

Power Comparison Test. The power needed to run our light source was recalibrated in order to create a new ratio. Because we were converting 120 volts to 2 volts for the LEDs, a resistance was needed which in turn produced wasteful heat. This was taken into account in order to be consistent with the G.E. light sources which are also run off of 120 volts. The new ratios for our system are calculated below and are compared to the other light sources discussed previously. As one can see, the combination of the LEDs with the blue fluorescent light provides a much higher effective light spectrum to wattage ratio. The metal halide comes in second with half our design's ratio.

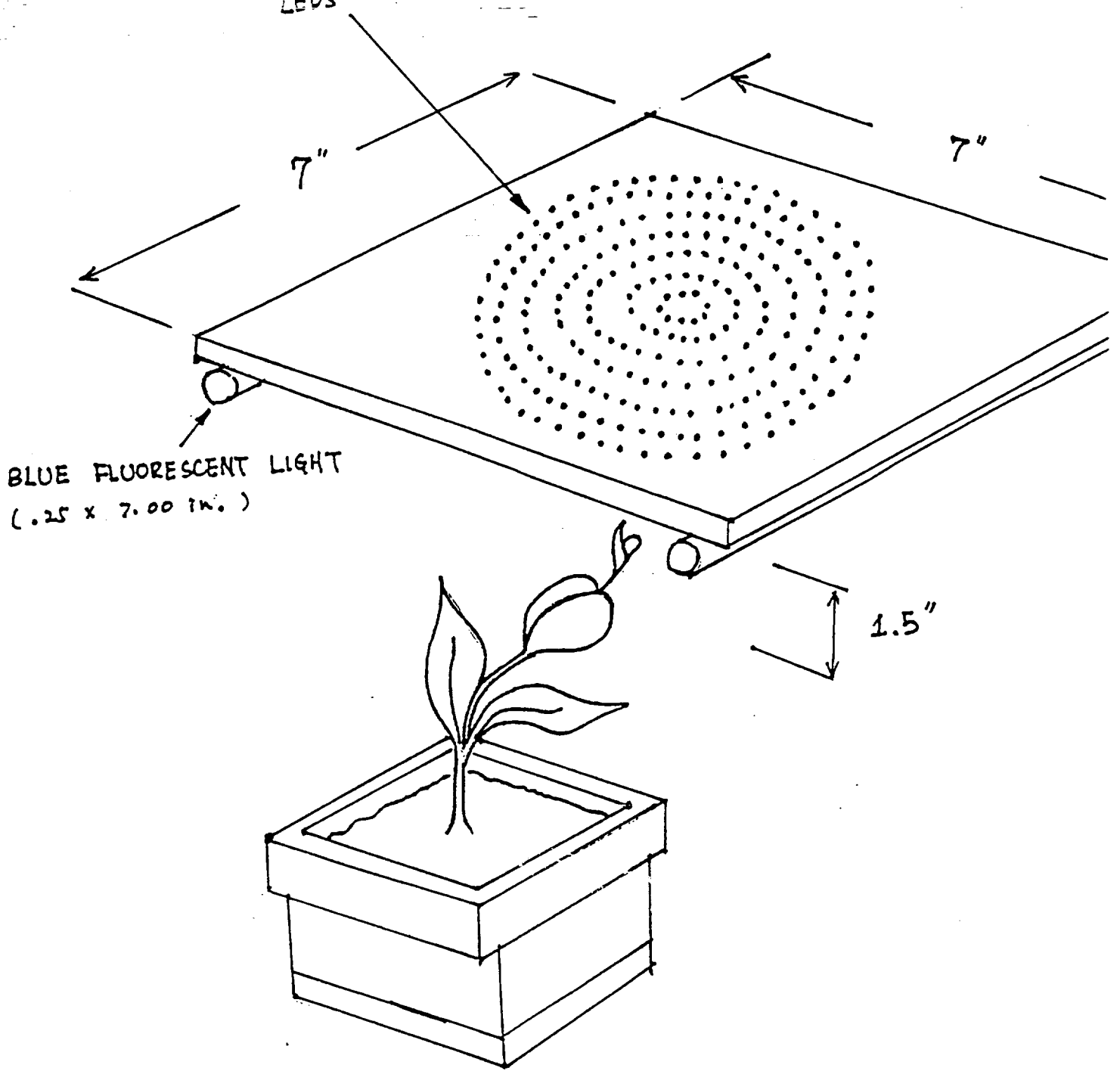
Table 3. New ratios with 120 volts input.

Light Sources	Ratios (Lumens/Watt)
Gro&Show	7.5
Metal Halide	38.2
HPS (LU 400)	14.5
HPS (LU 1000)	17.3
Our Light Design	78.8

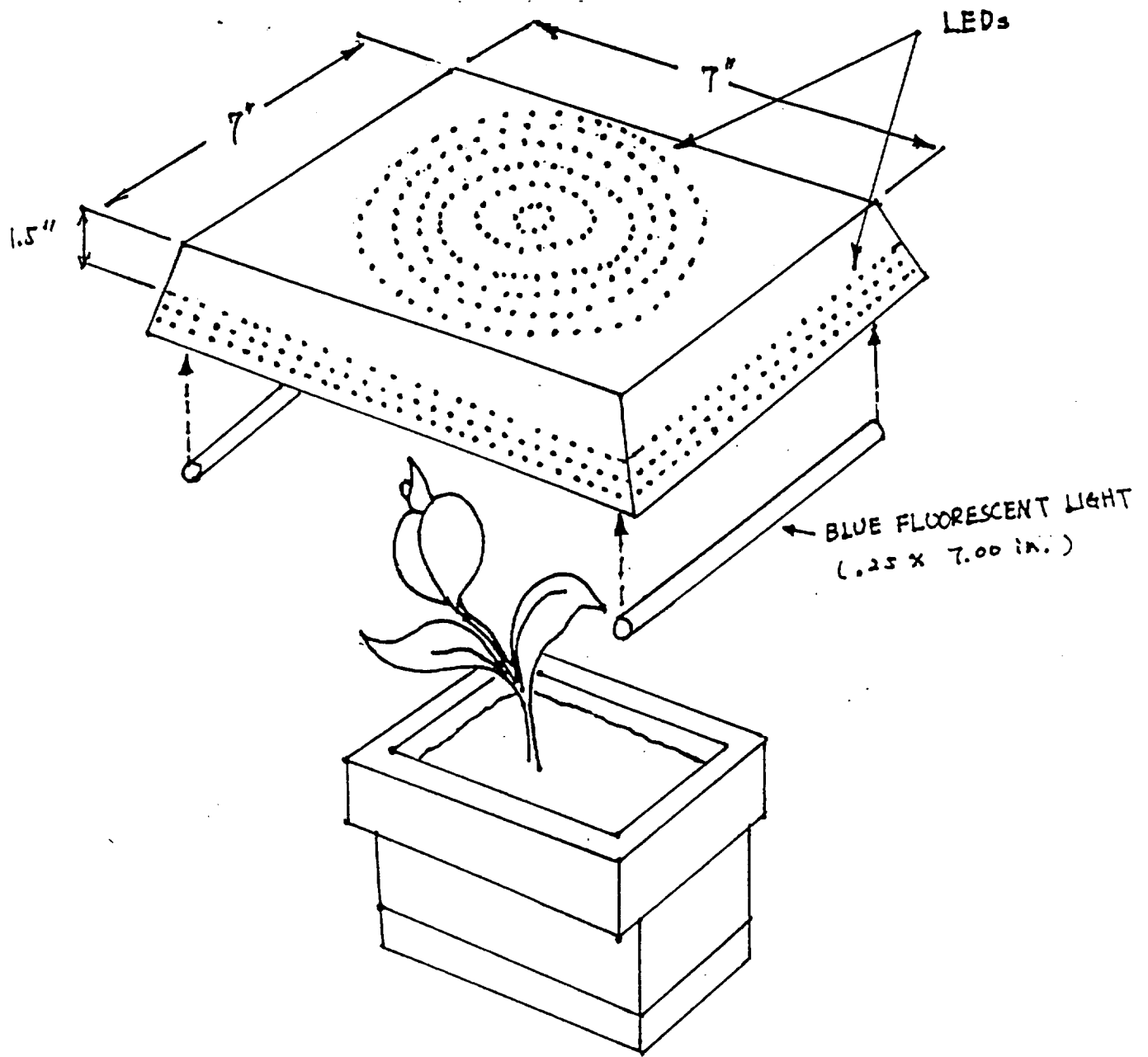
CONCLUSIONS

Light can be provided by various different kinds of sources for plants. However, plants absorb different wavelengths and quantities of light most of which is located in the blue and red areas of the spectrum. Our group decided to use an LED (660 nm) and a miniature blue fluorescent light (435 nm) due to the fact that their efficiency ratios were higher than other light sources compared. Two different types of tests were performed. The first was to show the variation of intensities as the distance away from the design was increased. The LEDs provided a constant intensity while the fluorescent leveled off at a higher height. The second test was to compare the actual power our light source was using with the power the other sources used. Our new lumens to watt ratio for our design was twice as high as the next highest ratio (metal halide). Other testing that could be conducted could include using light filters in order to see if the effective spectrum we calculated from the manufacturer's information was indeed the true light spectrum being produced.

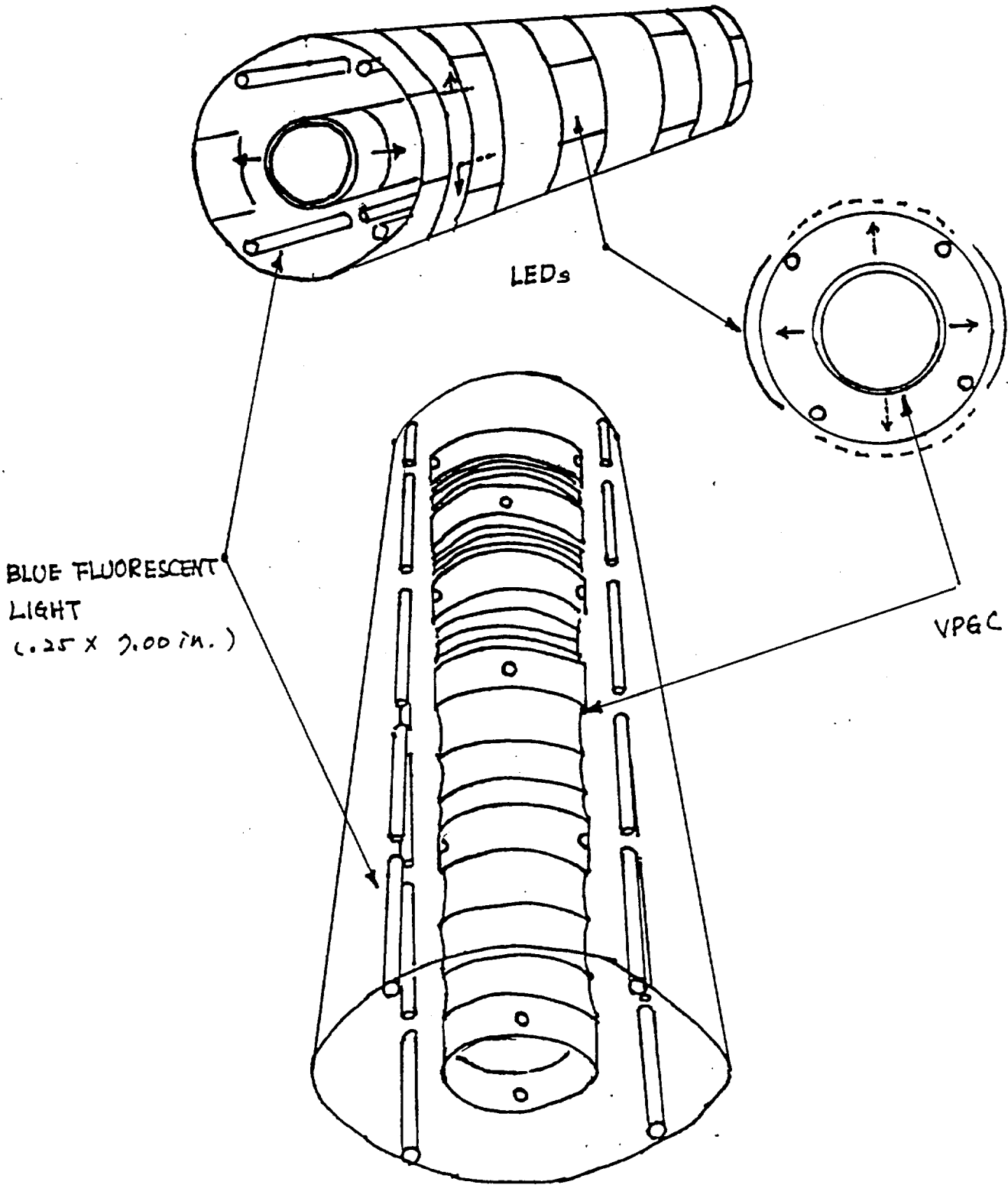
APPENDIX 1



Concept 1



Concept 2



Concept 3

WORKS CITED

Attridge, T. Light and Plant Responses. Edward Arnold, New York, 1990.

Napier, Richard. The Evaluation of a Light Emitting Diode. M.S. Thesis, University of Florida, 1988.

"Photosynthesis". Encyclopedia Britannica. Vol. 18, 1991.

Senger, Horst. Blue Light Response Phenomena and Occurrence in Plants and Microorganisms. CRC Press, Vol. 1 and 2, Boca Raton, FL, 1987.

Senger, Horst. Blue Light Effects in Biological Systems. Springer-Verlay, New York, 1984.

Senger, Horst. The Blue Light Syndrome. Springer-Verlay, New York, 1980.

Williams, E. Luminescence and the LED. Pergamon Press, New York, 1978.

